UCRL 710
Cy. 2

UNIVERSITY OF CALIFORNIA

Radiation Laboratory

TWO-WEEK LOAN COPY

This is a Library Circulating Copy which may be borrowed for two weeks. For a personal retention copy, call Tech. Info. Division, Ext. 5545

BERKELEY, CALIFORNIA

DISCLAIMER

This document was prepared as an account of work sponsored by the United States Government. While this document is believed to contain correct information, neither the United States Government nor any agency thereof, nor the Regents of the University of California, nor any of their employees, makes any warranty, express or implied, or assumes any legal responsibility for the accuracy, completeness, or usefulness of any information, apparatus, product, or process disclosed, or represents that its use would not infringe privately owned rights. Reference herein to any specific commercial product, process, or service by its trade name, trademark, manufacturer, or otherwise, does not necessarily constitute or imply its endorsement, recommendation, or favoring by the United States Government or any agency thereof, or the Regents of the University of California. The views and opinions of authors expressed herein do not necessarily state or reflect those of the United States Government or any agency thereof or the Regents of the University of California.

UCRL 710

Copy 1.

UNCLASSIFIED

I. Phenomenological Interpretation of High Energy Proton-Proton Scattering
II. Meson Production by Protons on Deuterons

By

Henry Pierre Noyes
A.B. (Harvard University) 1943

DISSERTATION

Submitted in partial satisfaction of the requirements for the degree of

DOCTOR OF PHILOSOPHY

in

Physics

in the

GRADUATE DIVISION

of the

UNIVERSITY OF CALIFORNIA

Approved:

.....

.....

.....

Committee in Charge

Deposited in the University Library .....
Date Librarian

I. Phenomenological Interpretation of High Energy Proton-Proton Scattering

INTRODUCTION

In this report we shall attempt to fit the proton-protons scattering data at 32[1][2] and 350 Mev[3] by the use of static nuclear potentials. This description is phenomenological and as such may be considered a sequel to the report concerned with determining the n-p interaction from the scattering data at 40, 90,[4][5][6] and 280 Mev.[7]

The success that was obtained in the n-p system would seem to be sufficient grounds for expecting that p-p scattering would likewise be interpretable by means of static potentials. In fact we might be tempted to predict the p-p nuclear potential from our knowledge of the n-p potential as determined by the high energy scattering. This prediction could be made either on the hypothesis that the nuclear potential is charge independent (i.e. depends only upon whether the two particles are in a singlet or triplet spin state), or in terms of an attempt to explain the saturation of nuclear forces.

If we were to follow the first assumption (the so-called symmetry hypothesis) there would be no free parameters entering the p-p theory, since the results of the n-p experiments are quite definite. For both singlet and triplet states these experiments show that there are no (or very small) odd parity forces. Therefore on the basis of charge symmetry one might expect that the n-p and p-p scattering would be quite similar. This is in obvious disagreement with the experimental results as is seen in Figure 1.

In order to better understand the prediction of the charge symmetric theory we must consider in more detail the fundamental differences between n-p and p-p

scattering. Firstly, for 32 Mev protons the coulomb repulsion is dominant in the scattering at angles less than 20°. Between 20° and 40° or 50° the angular variation is governed by the nuclear-coulomb interference terms. The remaining region around 90° is vitually the same as for simple nuclear scattering. Secondly, the p-p system, being composed of identical particles obeying the exclusion principle, has fewer states than the n-p system. Specifically only even parity singlet states and odd parity triplet states can be present. Thus scattering occurs only in ^1S, ^3P, ^1D, ^3F... states, and the charge symmetric theory predicts the virtual absence of triplet scattering. The n-p system, on the contrary, has scattering from both singlet and triplet even parity states so that a direct comparison must be justified. In order to learn what part of the complete n-p scattering is singlet scattering we must recall that in order to lead to the low total n-p cross section the singlet range must be greater than 2×10^{-13}cm. This gives an angular distribution for the singlet cross section that has an even higher ratio of $\frac{\sigma(180^\circ)}{\sigma(190^\circ)}$ than the complete scattering from both states, making a direct comparison of the relative angular variation of the complete n-p and p-p cross section possible in the region from 50° to 90°. Thus the 32 Mev p-p results show that the charge symmetry hypothesis is untenable.

Alternatively we could attempt to predict the p-p scattering by directing our attention to the phenomenon of the saturation of nuclear forces. The n-p experiments rule out the possibility of n-p repulsive forces of anything like the magnitude required to explain saturation. The low energy experiments show that the singlet p-p forces are attractive. Thus the only remaining way for the p-p forces to lead to saturation would be the existence of strong repulsive forces in the triplet state. Since the triplet scattering amplitude is antisymmetric, the scattering from a central triplet potential is zero at 90°. Hence such repulsive forces would lead to an angular cross section rising even more rapidly on either side of 90° than that predicted by the charge symmetric theory and are conclus-

ively excluded by the data.

Thus both the hypothesis of the charge independence of nuclear forces and the possibility of stron repulsive forces in the triplet p-p state such as seem to be required for the saturation of nuclear forces are already disallowed by the p-p scattering at 32 Mev. The 350 Mev scattering is even more strikingly anomalous (cf. Figure 1). The experiments indicate a nearly spherically symmetric distribution over the range from 41° to 90° having an absolute magnitude that is twice the maximum possible for S wave scattering alone. Since the n-p scattering at 280 Mev was in good agreement with a non-relativistic potential model it is difficult to accept this as a relativistic effect. Again both charge symmetry and repulsive triplet forces would lead to scattering stronly peaked at 0° and 180° and an order of magnitude lower in value at 90° than the observed p-p cross section, and are conclusively disproved. This scattering is superficially similar to classical hard sphere scattering. However, since the wavelength of 350 Mev protons is only three or four times shorter than the range of the attractive region that must surround and include such a sphere in order to explain the low energy results, the sphere cannot be made large enough to give classical hard sphere scattering at this energy. This point is discussed in more detail below.

In spite of the surprising divergence of the observed p-p scattering from that which had been expected previous to the experiments, it has proved possible to reconcile all the existing data with the scattering predicted from a static nuclear potential. This model consists of a shallow singlet potential and a highly singular triplet tensor potential. The main body of this paper is concerned with justifying this model.

In view of the apparently fundamental differences between the expected and the observed p-p scattering, and the various complicating factors in the analysis of

the data, we have devoted the first part of this report to a more or less qualitative discussion of p-p scattering. In this section we will give typical results for various potential models but will not discuss which radial dependence is to be preferred. Rather we wish to emphasize the salient features in the analysis in order to furnish a basis for understanding the calculations which follow in Part 2.

PART 1. QUALITATIVE DISCUSSION

It has been shown by many authors that the experiments below 14 Mev are compatible with S wave scattering alone[8] and that these experiments have determined only the scattering length and effective range.[9] This indicates that no one of the radial forms usually assumed is to be preferred. It need hardly be emphasized that the low energy experiments give little information concerning the interactions in states of higher angular momentum (especially the P state) other than putting upper limits on the magnitudes of the interactions in these states.

The n-p experiments at 40 Mev[4][6] have shown that there is scattering in the D state and little scattering in the P state, and that the magnitudes of these interactions could be determined. It was therefore expected that since the range of forces for the p-p system is comparable, the scattering would likewise occur primarily in the S, P and D states.

It was observed immediately, as has been pointed out in the experimental papers,[1][2] that the data was in good agreement with that predicted by S wave scattering alone. This is in definite disagreement with the scattering predicted by the usual potential models. The reason is that the S state interaction completely specifies the entire singlet interaction, and in particular the effective range is so long that the D wave predicted at this energy is incompatible with the experimental results. (It would of course be possible to choose a potential that would give only S scattering at 32 Mev, but the effective range of such a potential

would then be much too short to fit the low energy region.)

If we consider in detail the predictions of the usual models we find that even for the most cut off potential (the square well) the D phase shift is already too large (0.77°), and as is to be expected the more long-tailed Yukawa potential has an even larger D phase shift (1.4°). The adverse effect of such D phase shifts on the angular distribution can be readily seen by reference to the second panel of Figure 2. The origin of this effect is destructive interference between S and D wave scattering in the region around 90°. This interference term is proportional to $\sin \delta_S \sin \delta_D \cos (\delta_S - \delta_D) P_2$. ($P_2(\cos \theta) = 3/2 \cos^2 \theta - 1/2$.) The usual models predict positive values for δ_S and δ_D, so that this term has a minimum at 90° as is observed in the n-p scattering but not in the p-p case. (Figure 2 also demonstrates that the coulomb scattering has little effect in the region from 50° to 90° and hence cannot alter this conclusion.)

The central triplet scattering amplitude being antisymmetric leads to a cross section that is zero at 90°, and since there is no interference with the singlet state it can only add to the rise away from 90°. Therefore scattering in this state will increase the discrepancy between the predictions made from the central force model and the experiments. Alternatively we can see this directly from the fact that the P scattering is proportional to $\sin^2 \delta_P \cos^2 \theta$, showing that the $\cos^2 \theta$ term must have a positive coefficient. These effects are illustrated in the third panel of Figure 2.

In order to explain the 32 Mev data, we require a model that would predict essentially spherically symmetric scattering in the absence of the coulomb field. We have already seen that central force scattering predicted by monatonically decreasing potential models of the usual radial form is in qualitative disagreement with experiment. Conceivably a more complicated radial dependence, such as a repulsive lip on a square well, could lead to negligible D phase shifts at

32 Mev. Attempts to build such models have been unsuccessful because they have effective ranges too short to fit the low energy data. In view of the straightforward interpretation of the n-p scattering and the inherent difficulty of using such a model to fit the 350 Mev data, it did not appear profitable to pursue such models any further.

The remaining alternative, within the framework of the potential picture, is the possibility that the D wave is masked by the scattering from tensor forces in the triplet state. A favorable result is predicted by the use of the Born approximation to compute the scattering (cf. Figure 3). (The Born approximation is valid for the P waves since the centrifugal barrier reduces the effect of the nuclear potential to a small perturbation.) The scattering computed this way is peaked at 90° and hence can add to the singlet cross section, which dips at 90°, to give an almost flat nuclear cross section. When the coulomb effects are included the resulting angular distribution is quite similar to S wave scattering (cf. Figure 4). Thus a proper choice of range and depth for the tensor potential can lead to agreement with the experiments. (An alternative way of understanding why the scattering can have a finite value at 90° even though it takes place in odd states is that the tensor force brings about a change in angular momentum, and tesseral harmonics other than the Legendre polynomials enter into the scattering amplitude. We can then see that the presence of $Y_1^1(\theta,\phi) = e^{i\phi} \sin \theta$ in addition to $Y_1^0(\theta,\phi) = \cos \theta$ leads to terms with a $\sin^2 \theta$ symmetry which when added to the $\cos^2 \theta$ symmetry terms in the singlet scattering could lead to a flat nuclear cross section.)

The 350 Mev data will first be analyzed independently of the 32 Mev data. The two models so derived will then be compared and reconciled. In order to further emphasize the anomalous nature of the high energy scattering, we note that if we assumed (arbitrarily) that there were no interactions in other than S states the predicted cross section would be spherically symmetric but ten or more times too

small. (Recall that even the maximum possible S wave cross section is only one-half the measured value.)

To analyze the situation in somewhat more detail we shall first consider the scattering that would result from the singlet state (since in this state the potential is completely specified by the assumption of a particular radial form). At 350 Mev the Born approximation is valid for central scattering and predicts the strong forward maximum illustrated in Figure 5. Alternatively we may view the problem in terms of a partial wave decomposition. Only the even Legendre polynomials are all 1 at 0° and 180° and alternate in sign at 90° (e.g. $P_o(90^o)=1$, $P_2(90^o)=-.5$, $P_4(90^o)=.375...$). Scattering by the usual monatonic potential models predicts that all phase shifts will have the same sign, so that there is constructive interference at 0° and 180° and destructive interference at 90°, giving a characteristic peaking of the angular distribution.

In order to obtain a flat cross section it would be necessary to require that phase shifts of even parity alternate in sign with increasing ℓ, resulting in a singlet cross section peaked at 90°. Then if this cross section were added to the central triplet cross section (which is always zero at 90°) a flat cross section would result. It does not appear possible, however, to find a singlet potential that will fit the scattering in the low energy region while at the same time predicting the required alternation in sign of the high energy phase shifts.

Before turning to the tensor models we will first consider the so-called hard sphere scattering which can have the required characteristic of giving phase shifts of alternating sign. At this wavelength of 0.5×10^{-13} cm it might appear superficially that a repulsive core in the central potential would give the desired result. However, it is found that when the effective range is fitted the repulsive core cannot extend more than 0.7×10^{-13} cm. Since the repulsive core is then not

much larger than the wave length of the proton, scattering occurs predominantly from the surrounding attractive region (which is required in order to give agreement with the low energy data). Such a model results in scattering in the high energy region similar to that predicted by more usual forms.

Again we must appeal to the tensor force in order to obtain agreement with the experimental data. In fact, if we recall that at 32 Mev we needed to add a triplet cross section that was peaked around 90° in order to mask the minimum in the singlet scattering we see that the situation at 350 Mev is very similar. We can again use the tensor force to obtain agreement, for in Born approximation scattering depends only on the combination kR where k is the wave number and R the range of the potential. That is, to produce the same scattering at a higher energy we need only contract the range by a factor that is the square root of the energy ratio, and adjust the depth to give the desired absolute magnitude to the scattering.

We therefore have indications of a tensor potential at both 32 and 350 Mev, and need only show that the requirements for the two cases are compatible. As the energy changes different regions of the potential will play the more dominant role. For example, at 32 Mev the potential region at distances of the order of 3 to 4×10^{-13} cm is most important while at 350 Mev the potential region at distances of the order of 1×10^{-13} cm has become important. By adjusting the range and depth of a tensor potential of any given radial form the predictions may be made to fit the 32 Mev experimental data. However at 350 Mev the P wave protons are able to explore the potential in to considerably shorter distances and it is necessary to have a stron interaction in this region in order to explain the very high 350 Mev cross section. The tensor scattering calculated for a singular potential in Born approximation as illustrated in Figure 3 illustrates these remarks. From the foregoing curves we can also see that an appreciable fraction of the 32 Mev scattering must be explained in terms of tensor forces if we wish to obtain

agreement with the high energy data. These curves further show that the tensor potential would probably have little effect below 10 Mev as the scattering amounts to less than 1 percent of the total scattering.

PART 2. CALCULATIONS

A. Methods

The singlet scattering from a potential of given radial form depending on two parameters is completely specified by the scattering length and effective range, which are determined by the scattering below 10 Mev. The general method of determining these parameters for a given radial dependence is discussed in detail by Blatt and Jackson.(9) The S scattering due to the nuclear potential alone at higher energies was calculated by direct numerical integration of the radial wave equation giving the S phase shift. The true S phase shift (in the presence of the coulomb field) was then obtained by treating the coulomb field as a perturbation according to the method of Chew and Goldberger.(10) The corrections amounted to approximately one degree or less. The D phase shift was calculated in Born approximation considering only the nuclear forces. (This method was checked by numerical integration in the case of the Yukawa potential, corrected for the coulomb field as above. The results at 32 Mev: 1.33° for the Born approximation, 1.45° for the exact nuclear calculation, 1.40° with the coulomb correction were assumed to be a satisfactory check.) Higher waves than the D were found to be negligible at 32 Mev.

As was shown in Part 1, it was not necessary to calculate any odd parity phase shifts due to central forces, but the tensor scattering was required. This was calculated using the exact values of the complex phase shifts, $\delta_{\ell}^{Jm_s}$, which enter into the tensor scattering. The result was in good agreement with that predicted by the Born approximation. There is a slight tendency for the Born approximation to predict somewhat larger angular variations than are found in the

more exact calculations. This can readily be understood in terms of the higher approximations of the Born approximation for then the scattering amplitude entering into each successive iteration (or each successive collision) is less well collimated than that entering the previous iteration, due to the scattering that occurs. A further small difference between the exact and the Born calculations occurs in the absolute magnitude, a tensor force taken with a postive sign (i.e. same sign as for the deuteron) always has less scattering in the exact calculation while the tensor force taken with a negative sign always has more scattering. A comparison between the exact predictions using the two signs and with the result of the Born approximation is afforded by reference to Figures 6 and 7.

The phase shifts arising from the coupled states entering the exact calculations were carried out by iteration (in the manner described in reference 6) after they had been cast in the form of coupled integral equations. In the case of the uncoupled states any of the methods usually applicable to central scattering may be used. We found that the integral variational expression was sufficiently accurate when the proper component of the plane wave was used as a trial function.

From the relatively small differences shown in Figures 6 and 7, we decided it was unnecessary to carry out the exact calculations for the nuclear part of the scattering. This is particularly so because we are able to offset any difference in absolute magnitude by choosing a slightly altered tensor depth (which will be determined only very roughly anyway from the present data). One difficulty with using the Born approximation is that the interference term (cf. Appendix 1, for a derivation of this term) between the nuclear and coulomb scattering identically vanishes, while the exact calculations at 32 Mev show that the P wave component of the nuclear scattering interferes appreciably with the coulomb scattering. We had therefore to compute two uncoupled phase shifts, δ_1^{00} and $\delta_1^{1\pm}$, and also iterate the coupled $^3P_2 + {}^3F_2$ state. The iteration process is rather tedious and

as the magnitudes of the phase shifts were small compared with the uncoupled phase shifts, we used the WKB approximation to obtain these phase shifts. We shall consider this approximation in more detail below: If the two independent solutions of the coupled equations have the asymptotic form

$$a_{\ell L} \sim a_{\ell L} \sin\left(kx - \frac{\ell\pi}{2} + \delta^J_{\ell L}\right),$$

where $L = \ell$ or $2J - 1$ depending upon which is the dominant state, then the nuclear phase shift may be easily shown to be given by

$$e^{2i\delta_\ell^{Jm_s}} = \frac{e^{i(\delta^J_{\ell\ell} - \delta^J_{L\ell})} - a^J_{\ell L} a^J_{L\ell} e^{i(\delta^J_{\ell L} - \delta^J_{L\ell}) + 2i\sqrt{\frac{(2L+1)}{(2\ell+1)}} \frac{\langle SLJm_s | SL0m_s\rangle}{\langle S\ell Jm_s | S\ell 0m_s\rangle} a^J_{\ell L} \sin(\delta^J_{\ell\ell} - \delta^J_{\ell L})}}{e^{-i(\delta^J_{\ell\ell} + \delta^J_{\ell L})} - a^J_{\ell L} a^J_{L\ell} e^{-i(\delta^J_{\ell L} + \delta^J_{L\ell})}}$$

where now $L = 2J - 1$ only, and we have set $a^J_{\ell\ell} = a^J_{LL} = 1$. In the case of the $^3P_2 + {}^3F_2$ state we have found that the Born approximation yields all quantities in this expression with the exception of δ^2_{11}, with sufficient accuracy. This we have computed by using the "equivalent central potential" (cf. reference 6) in WKB approximation and then applying the Born approximation to this potential to obtain the phase shift. δ^2_{11} is then the sum of two terms one of which is identical with that predicted by the Born approximation applied directly to the coupled equations and the other is of the nature of a correction term, and has the value

$$\Delta^2_{11} = \frac{36.6}{25.10} \frac{1}{kR} \int_0^\infty \left[xV_t(x)\right]^2 g_1{}^2(kx)\, dx$$

where we have written the tensor potential,

$$S_{12}V_t\left(\frac{r}{R}\right) = \left[\frac{3(\vec{\sigma}_1 \cdot \vec{r})(\vec{\sigma}_2 \cdot \vec{r})}{r^2} - \vec{\sigma}_1 \cdot \vec{\sigma}_2\right] V_t(x)$$

and

$$g_\ell(kx) = \sqrt{\frac{\pi kx}{2}}\, J_{\ell+\frac{1}{2}}(kx)$$

This procedure applied to the exponential and Yukawa radial dependences yields the coefficients of the interference terms within a few percent the coefficients determined from an exact calculation.

For the 350 Mev scattering the coulomb scattering was neglected and the singlet scattering was computed in Born approximation.

B. Results

The singlet cross sections for the square, exponential, and Yukawa models are shown in Figure 8. In each case the range and depth have been chosen to agree with Blatt and Jackson's low energy analysis. (The range and depth of the Yukawa potential and square well were determined independently by Chew and Goldberger before the results of Blatt and Jackson were available to us and agree with their assigned limits of error.) These parameters, together with the S and D phase shifts at 20 and 32 Mev, are collected in Table 1. Clearly there are significant differences in the angular distributions predicted by the various models. However, the magnitude of the D phase shift is always large enough to yield a curve that has a characteristically different shape than the experimental results in the region from 50° to 90° and too low in absolute value at 90°. The principal reason for this is the presence of a P_2 coefficient in the nuclear scattering arising from the interference between the S and the D waves.

The addition of a central P wave does not change the cross section at 90° as can be seen in Figure 9 where we have indicated the effect of adding positive and negative P phase shifts to the scattering predicted by the Yukawa model (which comes closest to fitting the 90° point). Clearly these curves do not agree with the experimental results, primarily because the nuclear cross section adds in the region from 50° to 90° (where the coulomb interference can be neglected).

It is seen from Table 1 that the D phase shift increases as the potential

becomes more long tailed. Since the D phase shift is too large even for the square potential we are forced to turn to more complicated radial forms, if we wish to account for the 32 Mev scattering by central interactions alone. Such a potential might be expected to be repulsive at long distances and attractive at short distances. Accordingly some attempts were made to annul the D wave by adding a repulsive lip to the square well. They met with little success, and having regard to the inherent difficulties implicit in such an approach when applied to attempt an explanation of the 350 Mev results, this approach was abandoned.

As discussed in Part 1, the effect of adding tensor force in the purely nuclear scattering is to produce a more nearly spherically symmetric angular distribution. The depth of the tensor potential and hence the amplitude of the scattering may be considered arbitrary, and must eventually be chosen to give agreement with the experimental data. In Figure 10 we have shown the result of adding the tensor scattering to the singlet state scattering. Clearly, if the same radial dependence is assumed to hold for both singlet and triplet states, approximate agreement may be obtained for the exponential potential with depth $V_t = \pm 50$ Mev. If we drop the restriction that the singlet and triplet potentials have the same radial dependence, it is clear that we can obtain better agreement, especially with the photographic data, by using the combination of square well for the singlet potential and Yukawa for the triplet (cf. Figure 11). (This combination utilizes a square well with the constant previously found for the singlet state and a tensor Yukawa well of range 1.25×10^{-13} cm and $V_t = \pm 26$ Mev.)

As was remarked in Part 1 tensor scattering at 32 Mev is only able to explore the tail of the potential, and consequently there is little uniqueness to the radial form which can be established from the 32 Mev data. To illustrate this we may consider the Born approximation. In this approximation the triplet differential

cross section (considering only the nuclear part) is proportional to

$$\sigma(\theta) \sim \left[C^2(\theta) + C^2(\pi - \theta) + C(\theta)\, C(\pi - \theta)\right]$$

where

$$C(\theta) = \frac{M}{h^2 K}\int_0^\infty V_t\left(\frac{r}{R}\right) g_2\,(Kr)\; r dr \quad , \quad K = 2k \sin\frac{\theta}{2}$$

Plots proportional to $C(\theta)$ are shown in Figure 12 as a function of $\alpha(2kR \sin\frac{\theta}{2})$ where α has been adjusted such that each model predicts almost the same scattering at 32 Mev. (Recall that the Yukawa potential with $R = 1.25 \times 10^{-13}$ cm gave a good fit to the data when combined with a shallow singlet potential.) From these plots we find that the following ranges are practically equivalent with respect to the 32 Mev scattering: $R=3.8\times10^{-13}$cm(square), $R=1.0\times10^{-13}$cm (exponential), $R=1.25\times10^{-13}$cm (Yukawa), $R=2.0\times10^{-13}$cm^2 $(\exp(-r/R)/(r/R)^2)$.

In the plots of $C(\theta)$ we have chosen the scale of the abscissa such that $\alpha(2kR \sin\frac{\theta}{2})=1$ for $\theta=90^\circ$ with a k corresponding to 32 Mev. For other angles we move up and down the abscissa according to $\sin\frac{\theta}{2}$ (e.g., to obtain the value for $C(180^\circ)$ at 32 Mev read the ordinate for an abscissa $\sqrt{2}$). The 90° point at other energies can be readily located as it is given at an abscissa which is the square root of the ratio of that energy to 32 Mev. Thus to obtain the value of $C(90^\circ)$ at 350 Mev read the ordinate at an abscissa of $\sqrt{\frac{350}{32}} = 3.30$.

As the energy increases a large difference in scattering occurs between the various models. The more shallow potentials give less scattering relative to that at 32 Mev. From the predictions of the various models for the singlet state it seems reasonable to allow approximately one-third of the nuclear scattering at 32 Mev to be of tensor origin. This gives a tensor cross section at 32 Mev which is comparable to the 350 Mev cross section in magnitude. We therefore see that the Yukawa and other even less concentrated (i.e., shallower) potentials do not predict a sufficiently high cross section at 350 Mev. It is therefore necessary to use the singular potential $\frac{e^{-r/R}}{\left(\frac{r}{R}\right)^2}$. The results for the complete cross section

at 350 Mev are compared in Figure 13. In order to indicate the essential features of the singular model, we again examine the curves in Figure 12. Clearly a square well of range 4×10^{-13} cm gives scattering of the correct form to fit the 32 Mev data, while a square well of range 1×10^{-13} cm gives 350 Mev scattering approximating to that predicted by the singular model. Thus by combining the shallow long range square well with a deep short range square well (which will not be explored by 32 Mev P wave protons) scattering approximating to that predicted by the singular model can be obtained.

C. Summary of Results

We have shown that the 32 Mev data can be fitted by means of two combinations of central and tensor force. These are: 1. The radial dependence is chosen the same for the central and tensor potential. The best fit is then with an exponential radial dependence of range 0.7×10^{-13} cm and with a tensor depth of $\pm$ 50 Mev. This model fits the counter data better than the photographic data. 2. The radial dependence is singular for the tensor potential and shallow and cut off for the central potential. The best fit is with a singlet square well of range 2.6×10^{-13} cm and with either a $V_t \exp(-r/R)/(r/R)$ radial dependence (with $R = 1.3 \times 10^{-13}$ cm and $V_t = \pm$ 26 Mev) or with a more singular potential $V_t \exp(-r/R)/(r/R)^2$ with $R = 2.0 \times 10^{-13}$ cm and $V_t = \pm$ 22 Mev. These combinations give better fits to the photographic data.

To fit the 350 Mev data we have shown that a very singular tensor force must be used, such as the $\exp(-r/R)/(r/R)^2$. The essential feature is that there must be a strong interaction in regions less than 0.5×10^{-13} cm.

The best fit of the combined data is therefore obtained by using the singular potential so adjusted that approximately one-third of the nuclear scattering at 32 Mev is accountable to tensor scattering.

It is clear that the present data are not sufficiently extensive to permit very precise specification of the radial forms; however, in the foregoing summary we have tried to emphasize the salient features of each model.

CONCLUSIONS

We have shown that it is possible to fit all the present p-p data by means of a shallow central potential for the singlet states and a singular tensor potential for the triplet states.

Quite apart from the potential models assumed, however, even the most casual comparison of the p-p data at 32 Mev with the n-p data at 40 Mev and, especially, a comparison of the 340 Mev p-p data with the 280 Mev n-p data shows that nuclear scattering is charge dependent. In particular, there is definite evidence in the n-p scattering data that large tensor scattering does not occur in the odd parity states.

It is possible that the radial dependences found necessary for p-p scattering would be acceptable for the n-p scattering even though the exchange behavior is different. A definite statement regarding this must await detailed calculations, however.

Finally we must take notice of the fact that no large repulsive forces have shown up in either the n-p or the p-p system of sufficient magnitude to account for nuclear saturation if saturation is to be predicted from two body forces. In both cases they would have been very easily detected, independent of the potential model assumed.

ACKNOWLEDGMENTS

This report was a joint publication by R. S. Christian and H. P. Noyes. The analysis was originally started by G. F. Chew and M. L. Goldberger, to whom the analysis of the low energy data to obtain the singlet potential parameters and the original demonstration that the observed 32 Mev scattering is incompatible with central force models is due. We are indebted to J. M. Blatt and J. D. Jackson for receipt of their forthcoming paper on the analysis of the low energy proton-proton scattering prior to publication. We owe more than can be stated to the inspiration and guidance of Professor Robert Serber throughout this research.

The work described in this paper was performed under the auspices of the Atomic Energy Commission.

APPENDIX I

The triplet cross section is given by

$$\frac{d\sigma}{d\Omega} = \frac{1}{3k^2} \sum_{m_s} \left(|R|^2 + RN_o^* + N_oR^* + \sum_{\mu} N_\mu^* N_\mu\right) \qquad (1A)$$

where

$$R = \frac{a}{2i}\left(\frac{e^{-ia\ln \sin^2\frac{\theta}{2}}}{\sin^2\frac{\theta}{2}} - \frac{e^{-ia\ln \cos^2\frac{\theta}{2}}}{\cos^2\frac{\theta}{2}}\right)$$

$$N_\mu = \sum_{J,\ell} \sqrt{4\pi(2\ell+1)}\; e^{2i(\sigma_\ell-\sigma_o)} \langle S\ell Jm_s | S\ell 0 m_s\rangle \langle S\ell Jm_s-\mu | S\ell\mu m_s-\mu\rangle \left(e^{2i\delta_\ell^{Jm_s}}-1\right) \bar{Y}_\ell^\mu(\theta,\phi)$$

$$a = e^2/kv$$

$$\sigma_\ell - \sigma_o = \tan^{-1}\frac{a}{\ell} + \tan^{-1}\frac{a}{\ell-1} + \ldots + \tan^{-1} a$$

$\bar{Y}_\ell^\mu(\theta,\phi)$ are the normalized tesseral harmonics and $\delta_\ell^{Jm_s}$ are the customary (complex) phase shifts that occur in tensor scattering (defined here in the presence of the Coulomb field).

In Equation (1A) the term involving $|R|^2$ is just the usual triplet Coulomb scattering and the terms $\sum_\mu N_\mu^* N_\mu$ are the usual nuclear scattering. The remaining terms represent the interference between nuclear and Coulomb scattering.

In our calculations of the tensor scattering the Coulomb modification of the nuclear phase shift was neglected as the expected order of magnitude of this modification was very small compared to the P phase shifts. Further the nuclear-Coulomb interference terms were calculated only for the P wave part of the nuclear scattering. These terms can then be written

$$\frac{9P_1(\cos\theta)}{2k^2}\left[\frac{\sin\alpha_1}{S^2} - \frac{\sin\beta_1}{C^2}\right]\left(\frac{1}{9}\sin^2\delta_1^{00} + \frac{1}{3}\sin^2\delta_1^{1\pm} - \frac{1}{6}A_1^{2\pm} - \frac{1}{9}A_1^{20}\right) \qquad (2A)$$

$$-\frac{9P_1(\cos\theta)}{2k^2}\left[\frac{\cos\alpha_1}{S^2} - \frac{\cos\beta_1}{C^2}\right]\left(\frac{1}{9}\sin\delta_1^{00}\cos\delta_1^{00} + \frac{1}{3}\sin\delta_1^{1\pm}\cos\delta_1^{1\pm} + \frac{1}{6}B_1^{2\pm} + \frac{1}{9}B_1^{20}\right)$$

where

$$\alpha_1 = a \ln S^2 + 2(\sigma_1 - \sigma_0)$$

$$\beta_1 = a \ln C^2 + 2(\sigma_1 - \sigma_0)$$

$$S^2 = \sin^2 \theta/2$$

$$C^2 = \cos^2 \theta/2$$

$$A_\ell^{Jm_s} = \mathrm{Re}(e^{2i\delta_\ell^{Jm_s}} - 1)$$

$$B_\ell^{Jm_s} = \mathrm{Im}(e^{2i\delta_\ell^{Jm_s}})$$

(2A) reduces to the expression given by G. Breit, C. Kittel, and H. M. Thaxton, Physical Review 57, 255, (1940) when the coupling between the $^3P_2$ and $^3F_2$ scattering is neglected.

APPENDIX II

The energy dependence of the foregoing tensor model of the proton-proton interaction has been investigated below 32 Mev. The angular distribution predicted by this model at 20 Mev is given in Figure 14 in comparison with pure S wave scattering and singlet scattering without the tensor force. Clearly the tensor model is closer to agreement with S wave scattering than at 32 Mev where this model and S wave scattering could not be distinguished by the experiments. Therefore the deviations from S wave scattering should be negligible at lower energies. The value of K calculated from the cross section at 90° is plotted in Figure 15 in comparison with Blatt and Jackson's best shape independent approximation[9] and central force models. The agreement in shape between our curve and that for a Yukawa S wave again demonstrates the pseudo-S character of the tensor model at lower energies. The points determined by Bruce Cork (C) confirm this prediction, which is not surprising as any smooth curve tangent to the straight line at low energies and passing through the experimentally determined point at 32 Mev would pass close to those points.

The experimental points in Figure 15 are:

MP	May and Powell, Proc. Roy. Soc. A190, 170 (1947)
M	Meagher, PhD Thesis, Univ. of Ill.
DOP	Dearnley, Oxley, and Perry, Phys. Rev. 73, 1290 (1948)
WC	Wilson and Creutz, Phys. Rev. 71, 337 (1947)
Wi	Wilson, Phys. Rev. 71, 384 (1947)
Wr	Wright, Private communication
WLRWS	Wilson, Lofgren, Richardson, Wright, Shankland, Phys. Rev. 72, 1131 (1947)
R	Rouvina, Private communication
PF	Panofksy and Filmore, Phys. Rev., July 1, 1950
RCJ	Richman, Cork and Johnston, Phys. Rev., July 1, 1950
C	Cork, Private communication

TABLE 1

Singlet phase shifts at 32 Mev for various radial forms adjusted to fit the low energy scattering.

Model	V_c	R	Phase Shift S	Phase Shift D
$V_c\left(\frac{r}{R}\right) = \begin{cases} V_c & r < R \\ 0 & r > R \end{cases}$	13.273 Mev	2.615×10^{-13} cm	41.99°	$.770^\circ$
$V_c\left(\frac{r}{R}\right) = V_c e^{-r/R}$	108.27 Mev	$.7088 \times 10^{-13}$ cm	47.54°	1.20°
$V_c\left(\frac{r}{R}\right) = \frac{V_c e^{-r/R}}{r/R}$	49.350 Mev	1.1417×10^{-13} cm	51.15°	1.40°

REFERENCES

(1) W. K. H. Panofsky and F. Fillmore, UCRL 481

(2) C. Richman, B. Cork, and L. Johnston, UCRL 482

(3) O. Chamberlain and C. Wiegand, UCRL 553

(4) J. Hadley, E. L. Kelly, C. E. Leith, E. Segrè, and H. F. York, Phys. Rev. 75, 351 (1949)

(5) K. Brueckner, W. Hartsough, E. Hayward, and W. M. Powell, Phys. Rev. 75, 555 (1949)

(6) R. S. Christian and E. W. Hart, Phys. Rev. (in press)

(7) E. Segrè (private communication)

(8) F. L. Yost, J. A. Wheeler, and G. Breit, Phys. Rev. 49, 174 (1936)

G. Breit, E. U. Condon, and R. D. Present, Phys. Rev. 50, 825 (1936)

G. Breit, H. M. Thaxton, and L. Eisenbud, Phys. Rev. 55, 1018 (1939)

L. E. Hoisington, S. S. Share, and G. Breit, Phys. Rev. 56, 884 (1939)

H. M. Thaxton and L. E. Hoisington, Phys. Rev. 56, 1194 (1939)

(9) J. Schwinger, Phys. Rev. 72, 742A (1947)

J. M. Blatt and J. D. Jackson, Phys. Rev. 76, 18 (1949); also Rev. Mod. Phys. 22, 77 (1950)

H. A. Bethe, Phys. Rev. 76, 38 (1949)

(10) G. F. Chew and M. L. Goldberger, Phys. Rev. 75, 1637 (1949)

FIGURE CAPTIONS

Figure 1. Comparison of n-p and p-p scattering data.

Figure 2. Effects of S, D, and P waves on 32 Mev scattering. The upper set of curves give the nuclear scattering. The lower set include the effects of coulomb forces.

Figure 3. Tensor scattering from a singular potential at various energies. The energies in Mev are given parametrically on the curves.

Figure 4. Effect of adding tensor scattering to the singlet scattering at 32 Mev. A. Nuclear scattering. B. Scattering including the effects of coulomb forces. The tensor scattering is that from a potential of exponential radial dependence ($R = .71 \times 10^{-13}$ cm, $V_t = \pm 50$ Mev).

Figure 5. Singlet scattering at 350 Mev as predicted for a potential having Yukawa radial dependence.

Figure 6. Comparison of exact and Born calculations for tensor force scattering at 32 Mev from a potential of Yukawa radial dependence ($R = 1.25 \times 10^{-13}$ cm).

Figure 7. Comparison of exact and Born calculations for tensor force scattering at 350 Mev from a potential of Yukawa radial dependence ($R = 1.25 \times 10^{-13}$ cm).

Figure 8. Singlet scattering at 32 Mev from potentials with various radial forms adjusted to fit the low energy scattering. Data taken from reference 2 (31.8 Mev).

Figure 9. P wave scattering added to the singlet scattering predicted by the Yukawa potential at 32 Mev.

Figure 10. Total scattering at 32 Mev by singlet and triplet tensor potentials of the same radial form. (The singlet potentials have range and depth adjusted to fit the low energy scattering.) A. Square B. Exponential C. Yukawa.

Figure 11. Singlet plus triplet tensor scattering at 32 Mev. The singlet potential is a square well ($R = 2.615 \times 10^{-13}$ cm, $V_c = 13.273$ Mev), and the tensor potential is a Yukawa potential ($R = 1.25 \times 10^{-13}$ cm, $V_t = \pm 26$ Mev). The experimental points are taken from reference (1) (at 29.4 Mev) and have been reduced in magnitude by 5 percent.

Figure 12. Born tensor scattering amplitude for various potentials. The abscissa scale has been adjusted so that all potentials will give the same angular distribution at 32 Mev as the Yukawa potential with $R = 1.25 \times 10^{-13}$ cm for a suitable choice of depth.

Figure 13. Complete cross section at 350 Mev for various tensor models adjusted to fit the 32 Mev data. The legend shows the tensor model used. Data taken from reference (3).

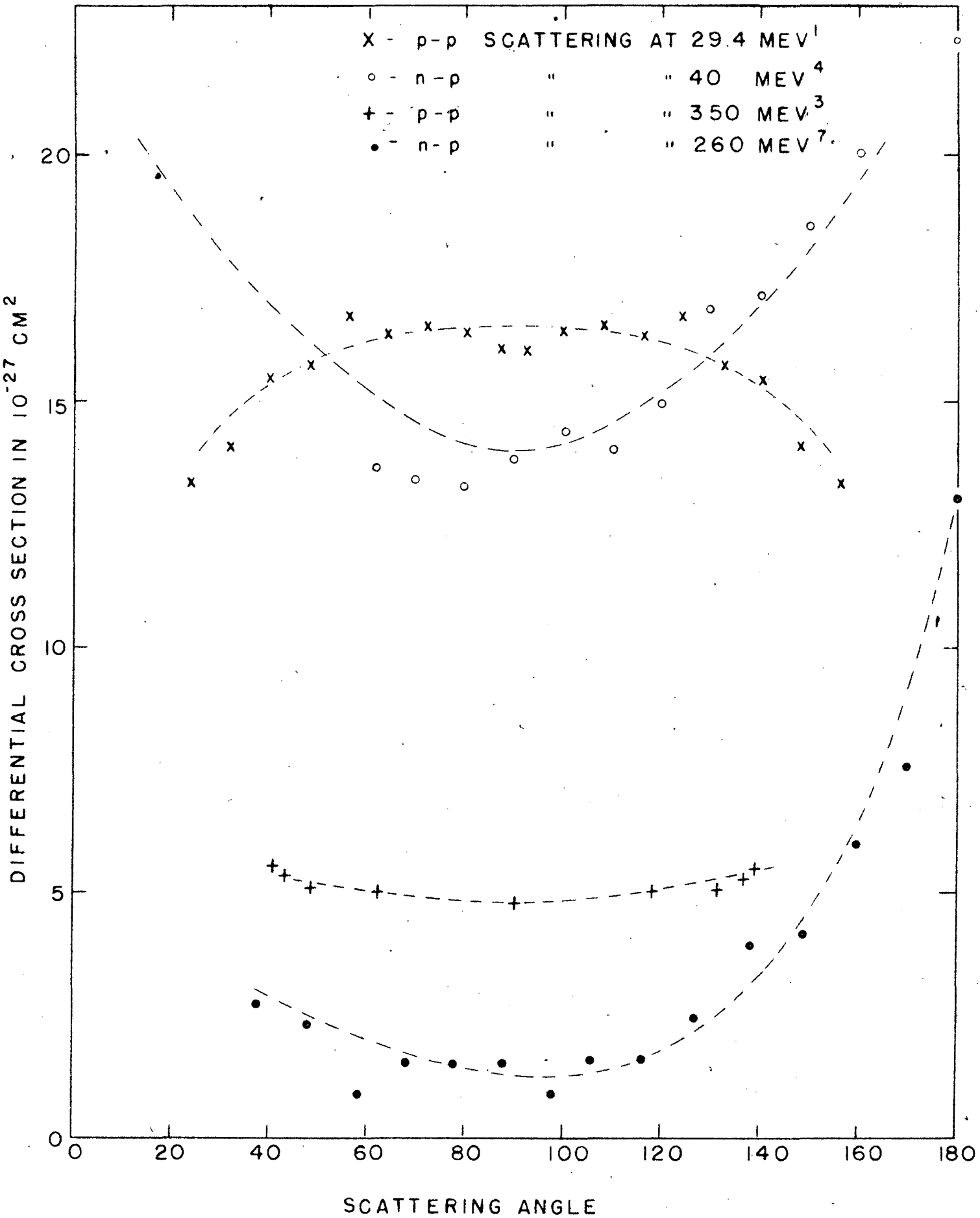
X - p-p SCATTERING AT 29.4 MEV[1]
○ - n-p " " 40 MEV[4]
+ - p-p " " 350 MEV[3]
• - n-p " " 260 MEV[7]
DIFFERENTIAL CROSS SECTION IN 10^{-27} CM^2
SCATTERING ANGLE
0
5
10
15
20
0
20
40
60
80
100
120
140
160
180

FIG. 1

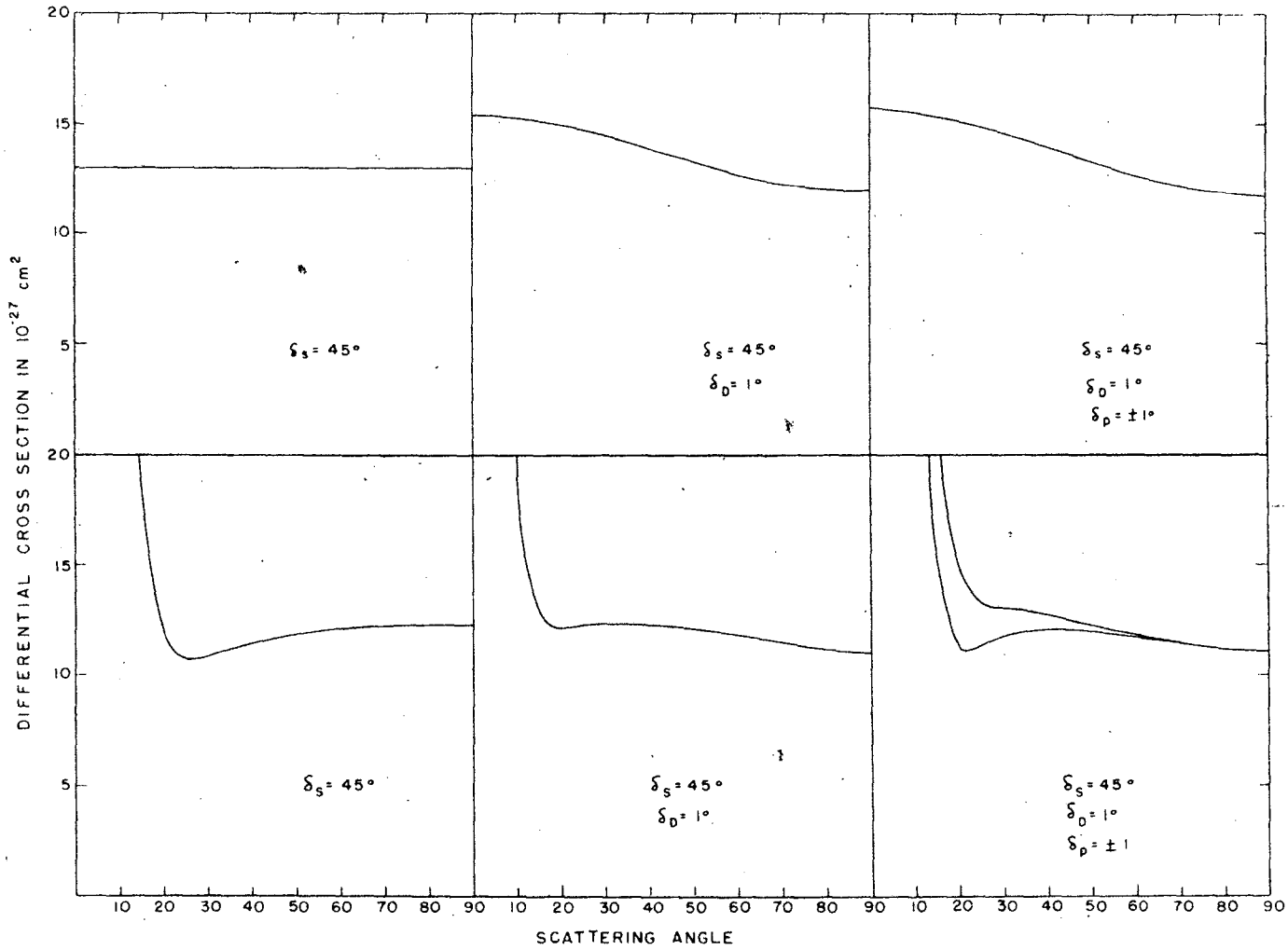
DIFFERENTIAL CROSS SECTION IN 10^{-27} cm^2
SCATTERING ANGLE
$\delta_s = 45°$
$\delta_s = 45°$
$\delta_D = 1°$
$\delta_s = 45°$
$\delta_D = 1°$
$\delta_p = \pm 1°$
$\delta_s = 45°$
$\delta_s = 45°$
$\delta_D = 1°$
$\delta_s = 45°$
$\delta_D = 1°$
$\delta_p = \pm 1$

FIG. 2

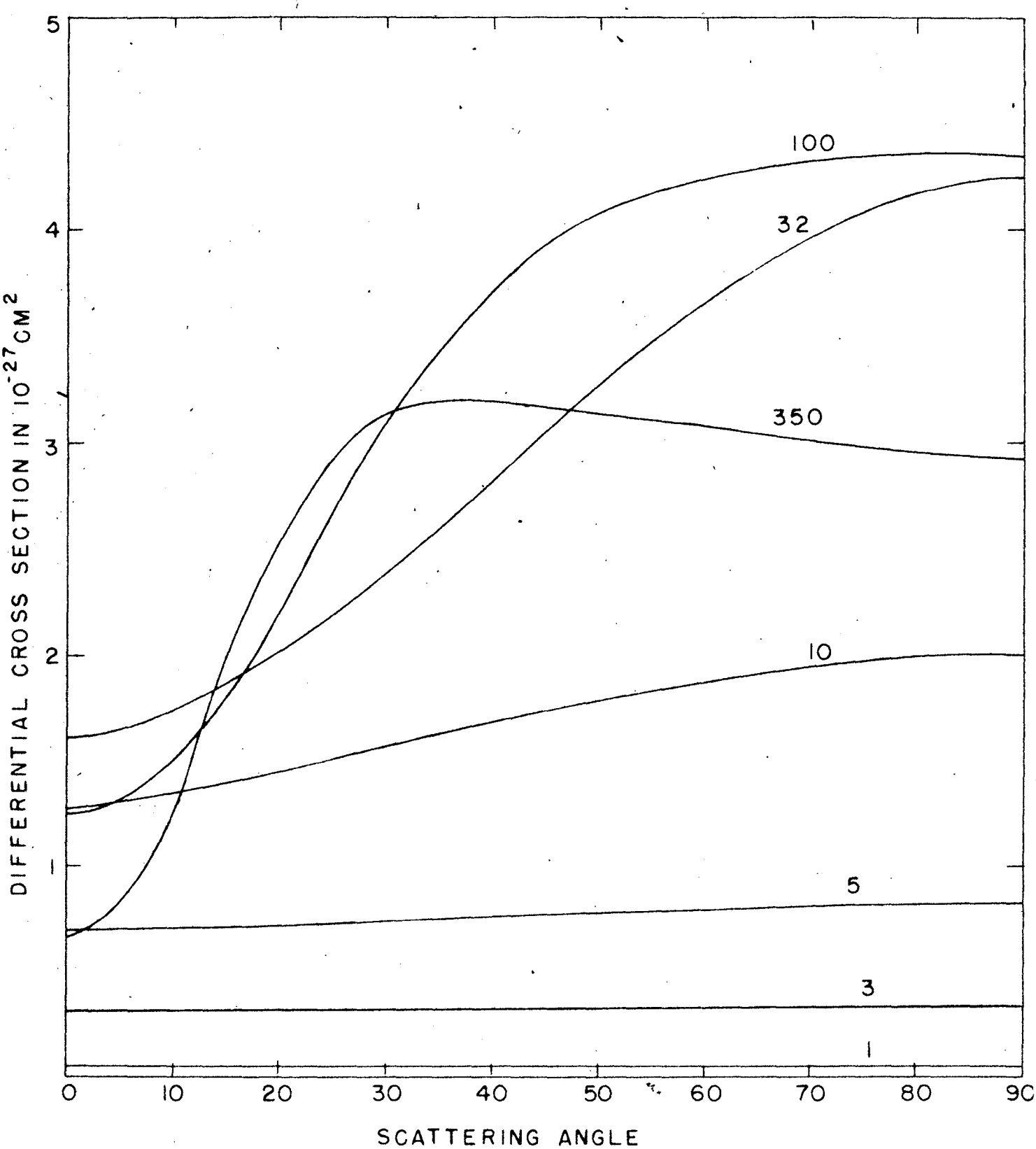
5
4
3
2
1
DIFFERENTIAL CROSS SECTION IN 10^{-27} CM^2
100
32
350
10
5
3
1
0
10
20
30
40
50
60
70
80
90
SCATTERING ANGLE

FIG. 3

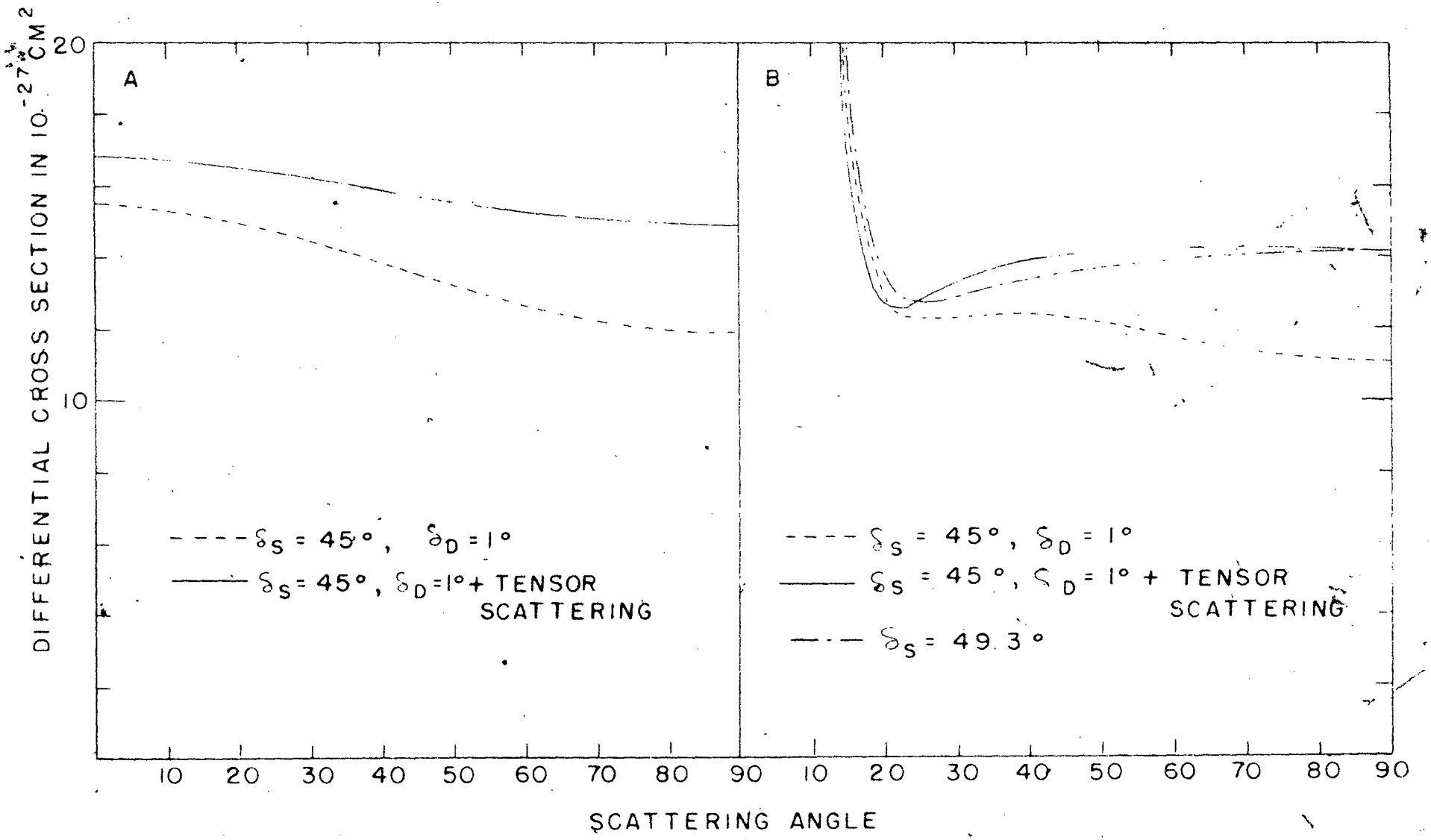
DIFFERENTIAL CROSS SECTION IN 10^{-27} CM^2
20
10
A
B
$\delta_S = 45°$, $\delta_D = 1°$
$\delta_S = 45°$, $\delta_D = 1°$ + TENSOR SCATTERING
$\delta_S = 45°$, $\delta_D = 1°$
$\delta_S = 45°$, $\delta_D = 1°$ + TENSOR SCATTERING
$\delta_S = 49.3°$
10 20 30 40 50 60 70 80 90
10 20 30 40 50 60 70 80 90
SCATTERING ANGLE

FIG. 4

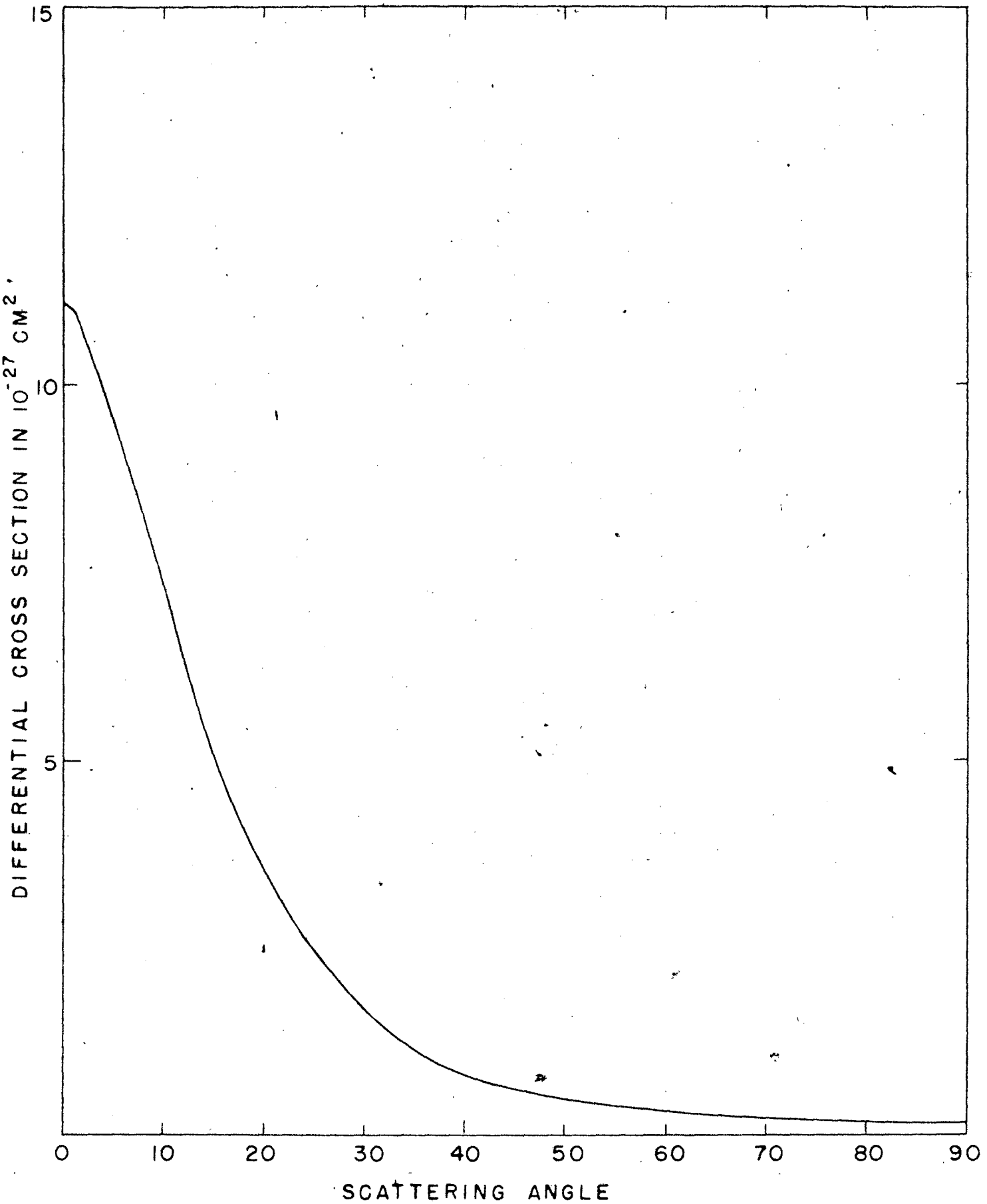
15
10
5
DIFFERENTIAL CROSS SECTION IN 10^{-27} CM^2
0
10
20
30
40
50
60
70
80
90
SCATTERING ANGLE

FIG. 5

14394-1

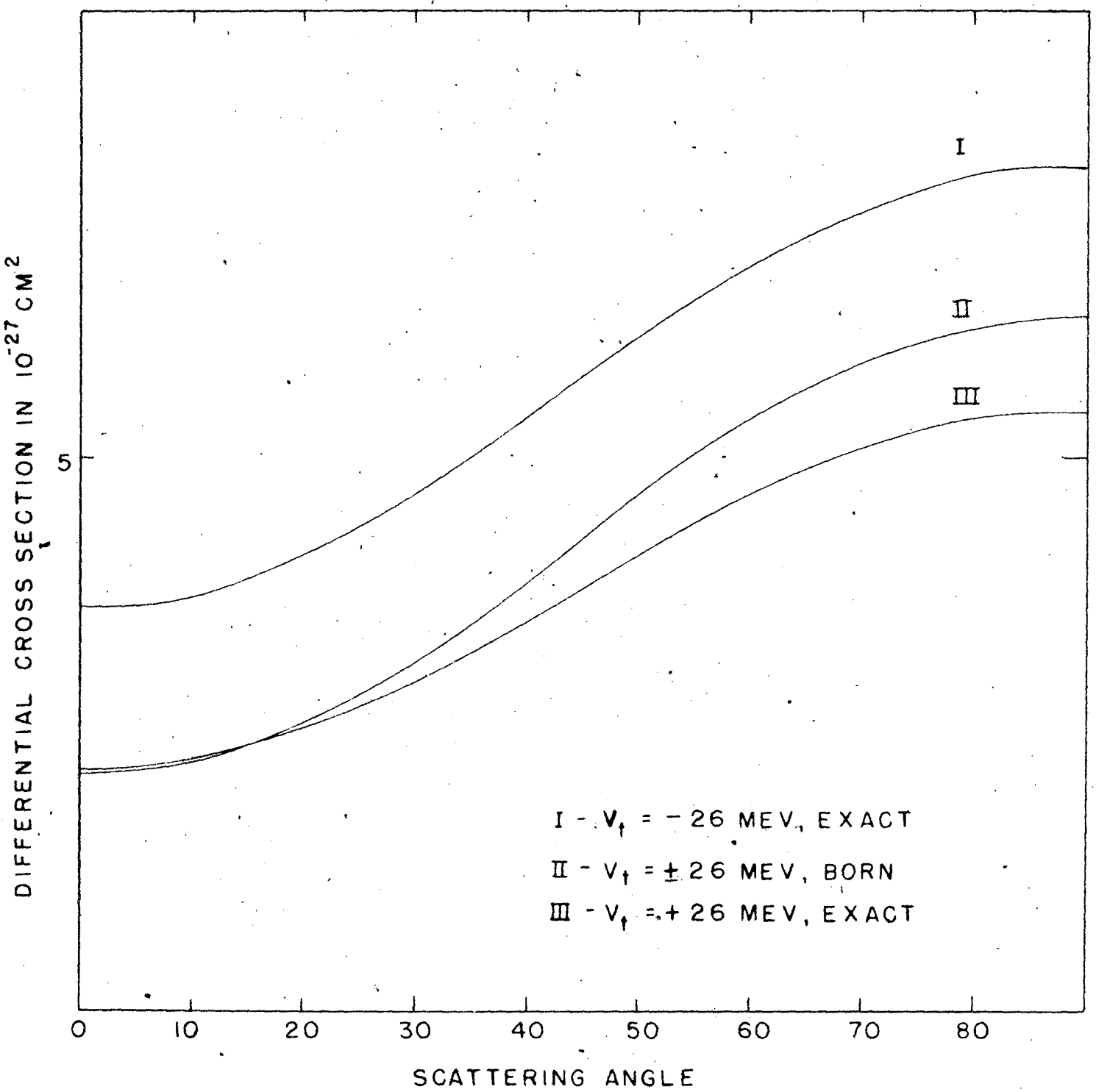
DIFFERENTIAL CROSS SECTION IN 10^{-27} CM^2
5
I
II
III
I - V_f = − 26 MEV, EXACT
II - V_f = ± 26 MEV, BORN
III - V_f = + 26 MEV, EXACT
0
10
20
30
40
50
60
70
80
SCATTERING ANGLE

FIG. 6

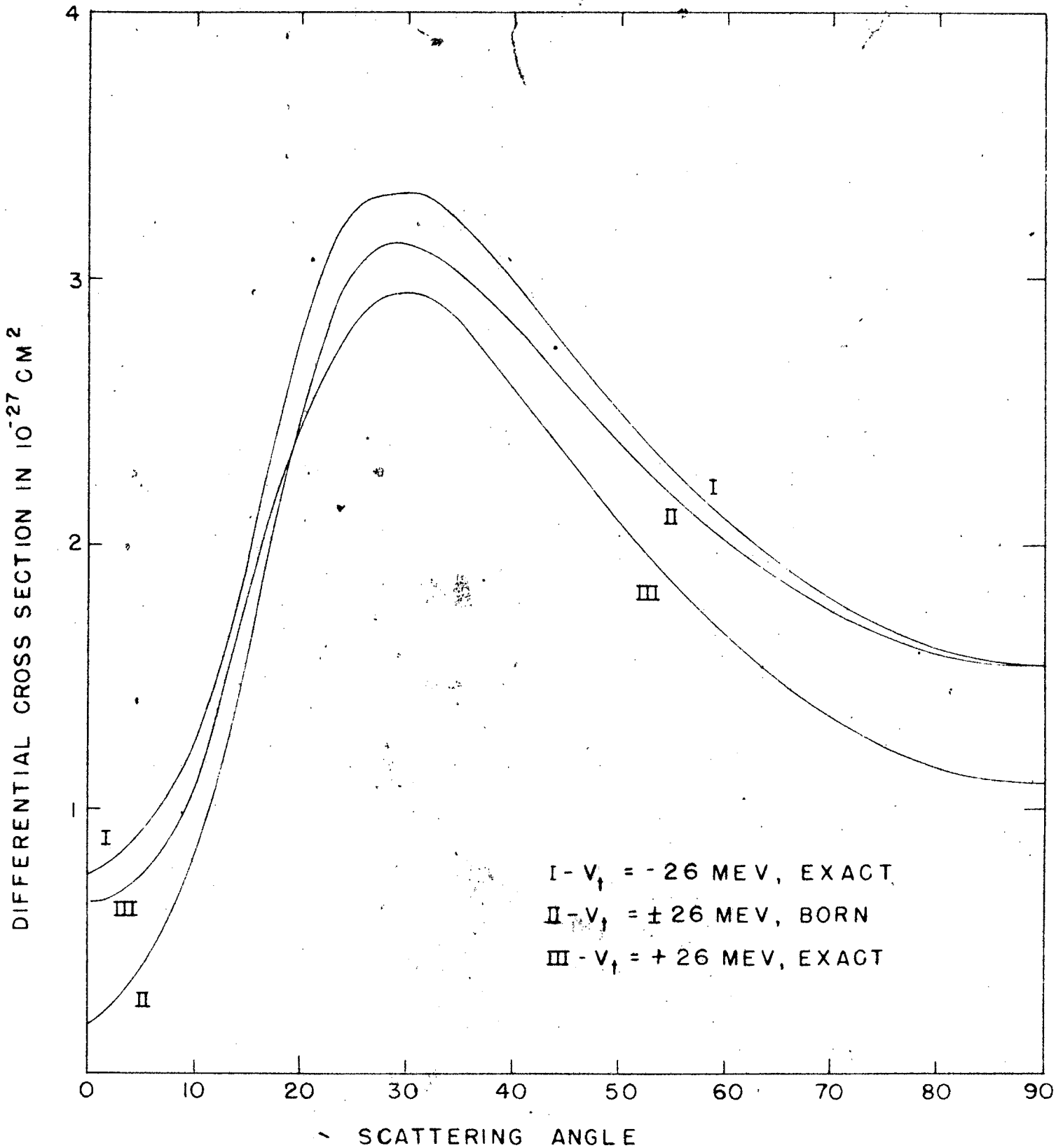
DIFFERENTIAL CROSS SECTION IN 10^{-27} CM^2
SCATTERING ANGLE
0
10
20
30
40
50
60
70
80
90
1
2
3
4
I
II
III
I - V_1 = - 26 MEV, EXACT
II - V_1 = ± 26 MEV, BORN
III - V_1 = + 26 MEV, EXACT

FIG. 7

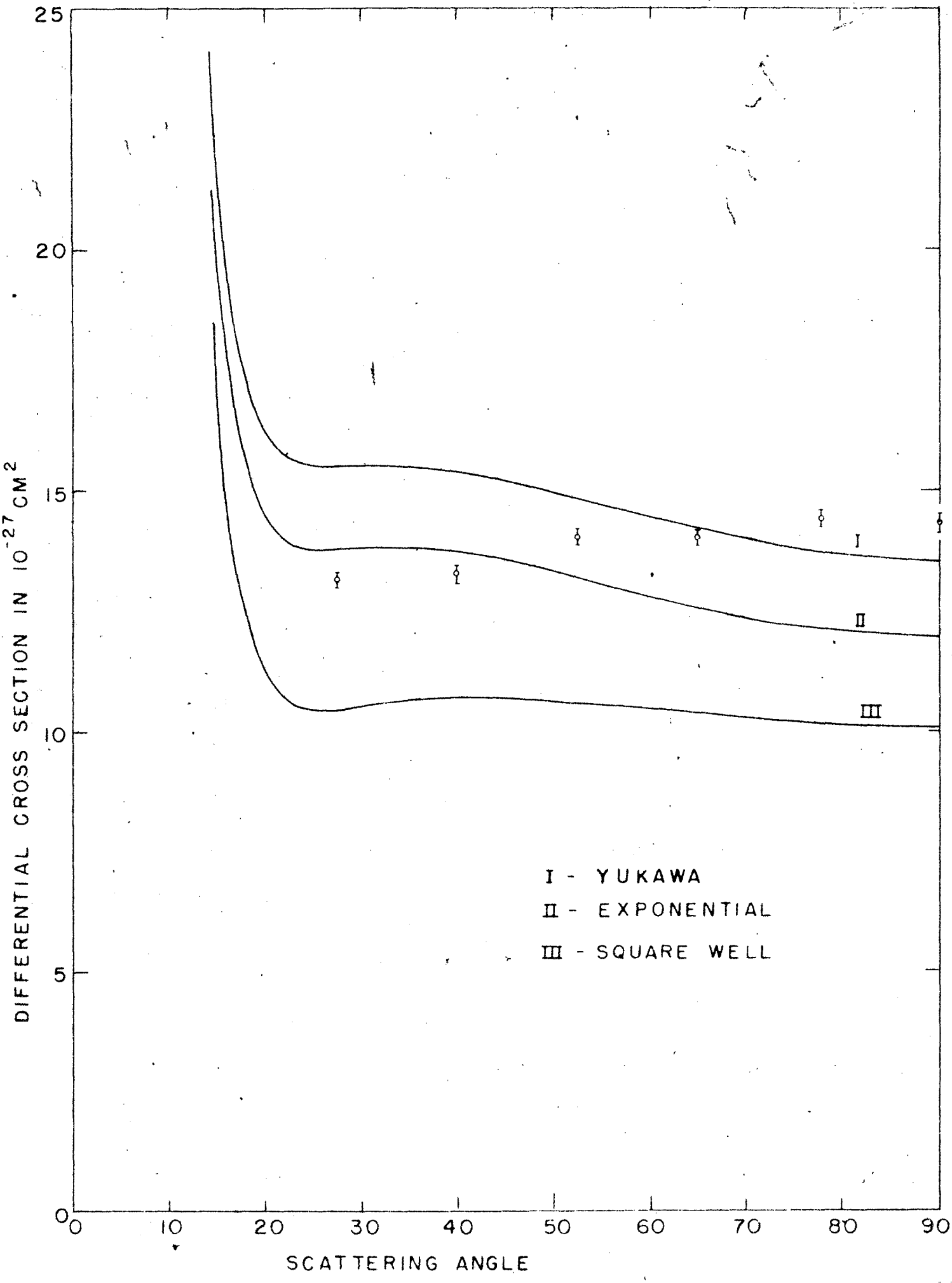
25
20
15
10
5
0
0
10
20
30
40
50
60
70
80
90
DIFFERENTIAL CROSS SECTION IN 10^{-27} CM^2
SCATTERING ANGLE
I
II
III
I - YUKAWA
II - EXPONENTIAL
III - SQUARE WELL

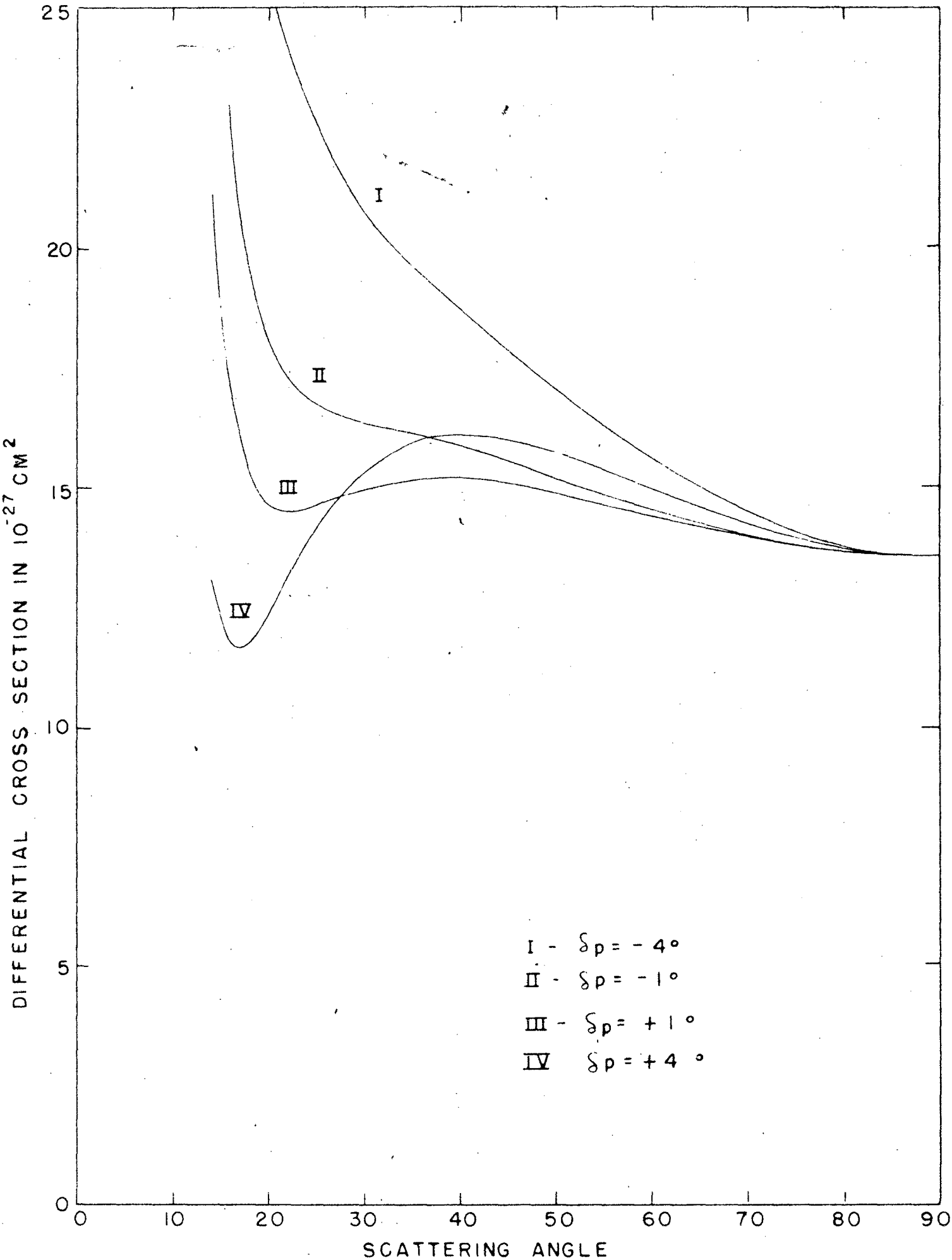
25
20
15
10
5
0
0
10
20
30
40
50
60
70
80
90
DIFFERENTIAL CROSS SECTION IN 10^{-27} CM^2
SCATTERING ANGLE
I
II
III
IV
I - $\delta p = -4°$
II - $\delta p = -1°$
III - $\delta p = +1°$
IV $\delta p = +4°$

FIG 9

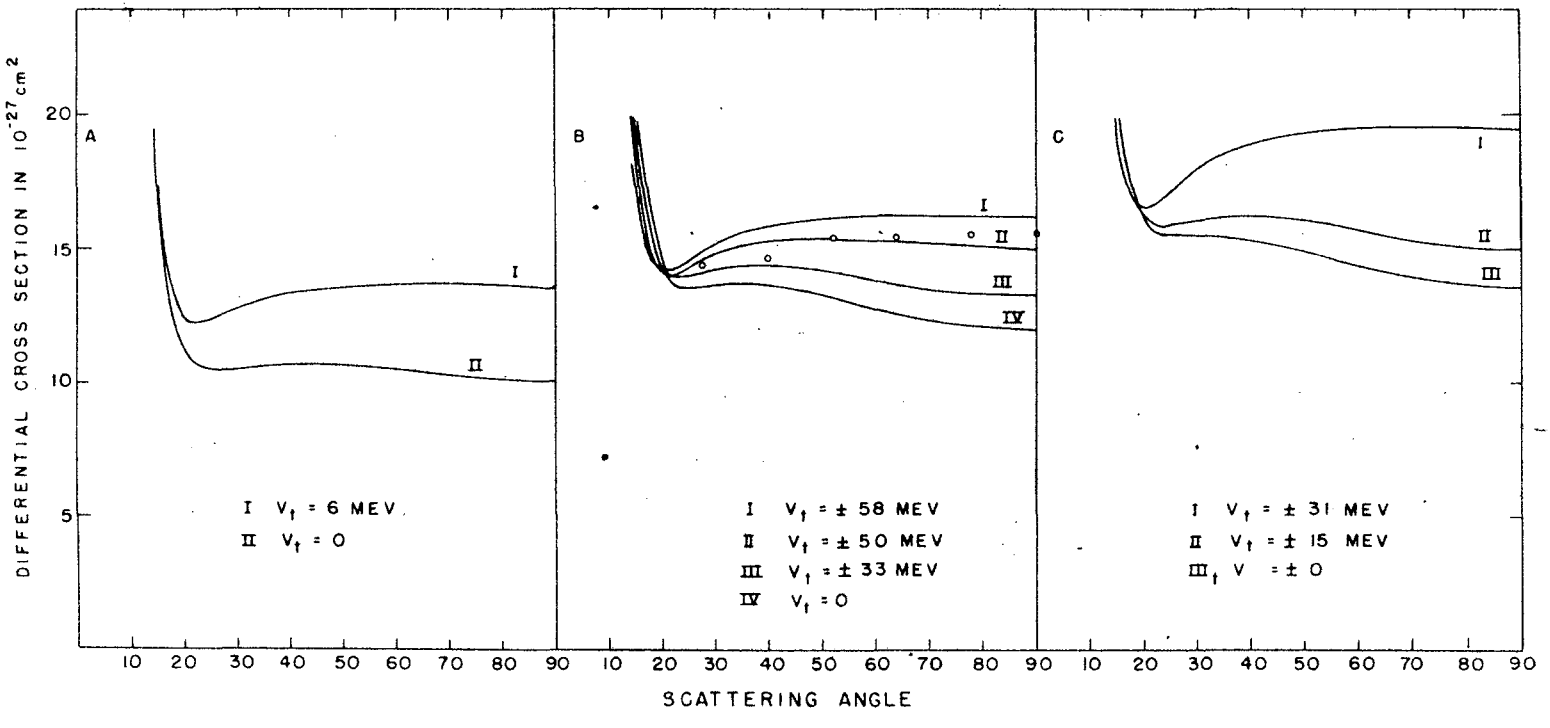
DIFFERENTIAL CROSS SECTION IN 10^{-27} cm^2
20
15
10
5
A
B
C
I
II
III
IV
I V_t = 6 MEV
II V_t = 0
I V_t = ± 58 MEV
II V_t = ± 50 MEV
III V_t = ± 33 MEV
IV V_t = 0
I V_t = ± 31 MEV
II V_t = ± 15 MEV
III V_t = ± 0
10 20 30 40 50 60 70 80 90
SCATTERING ANGLE

FIG. 10

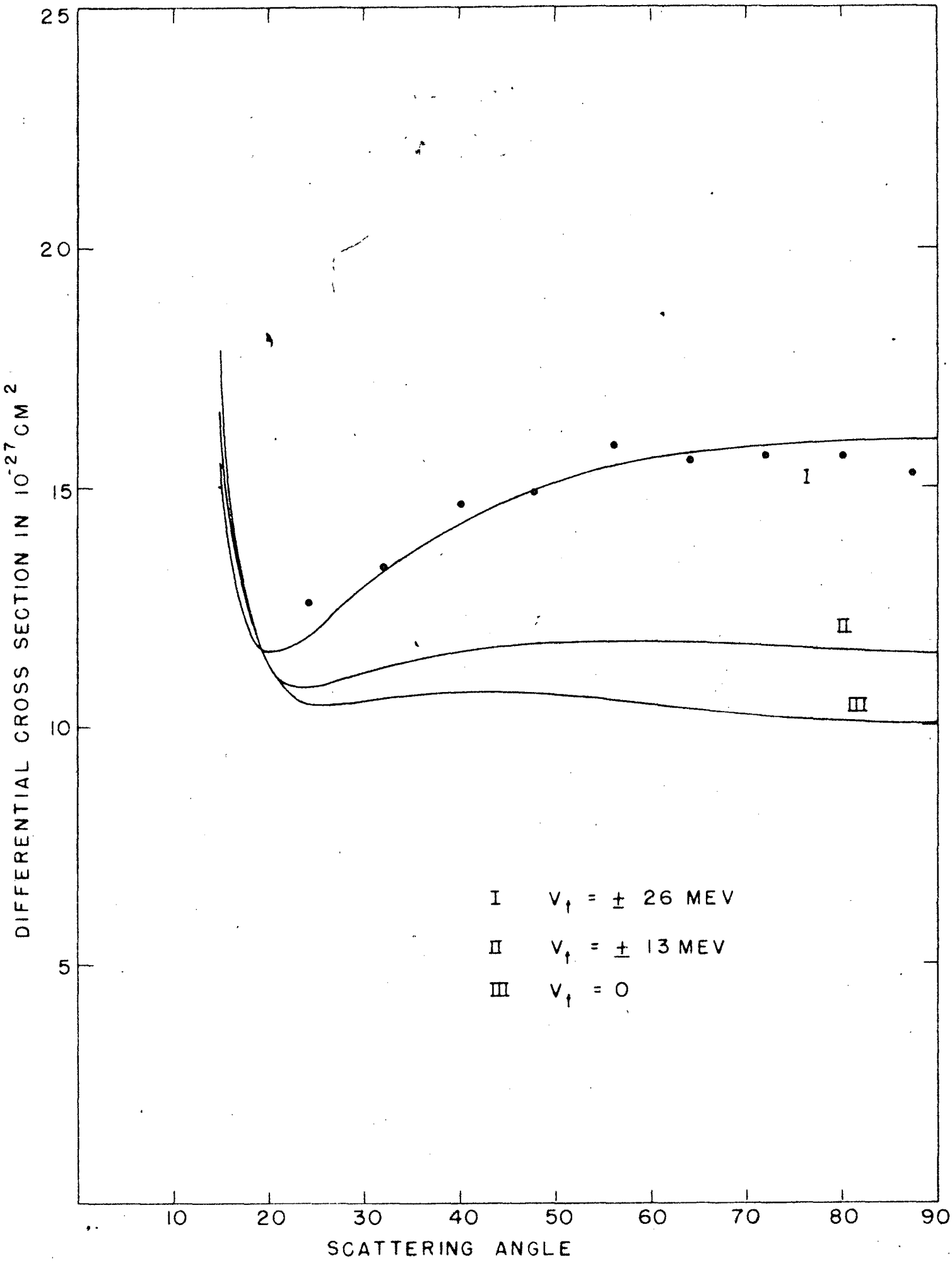

FIG. 11

14397-1

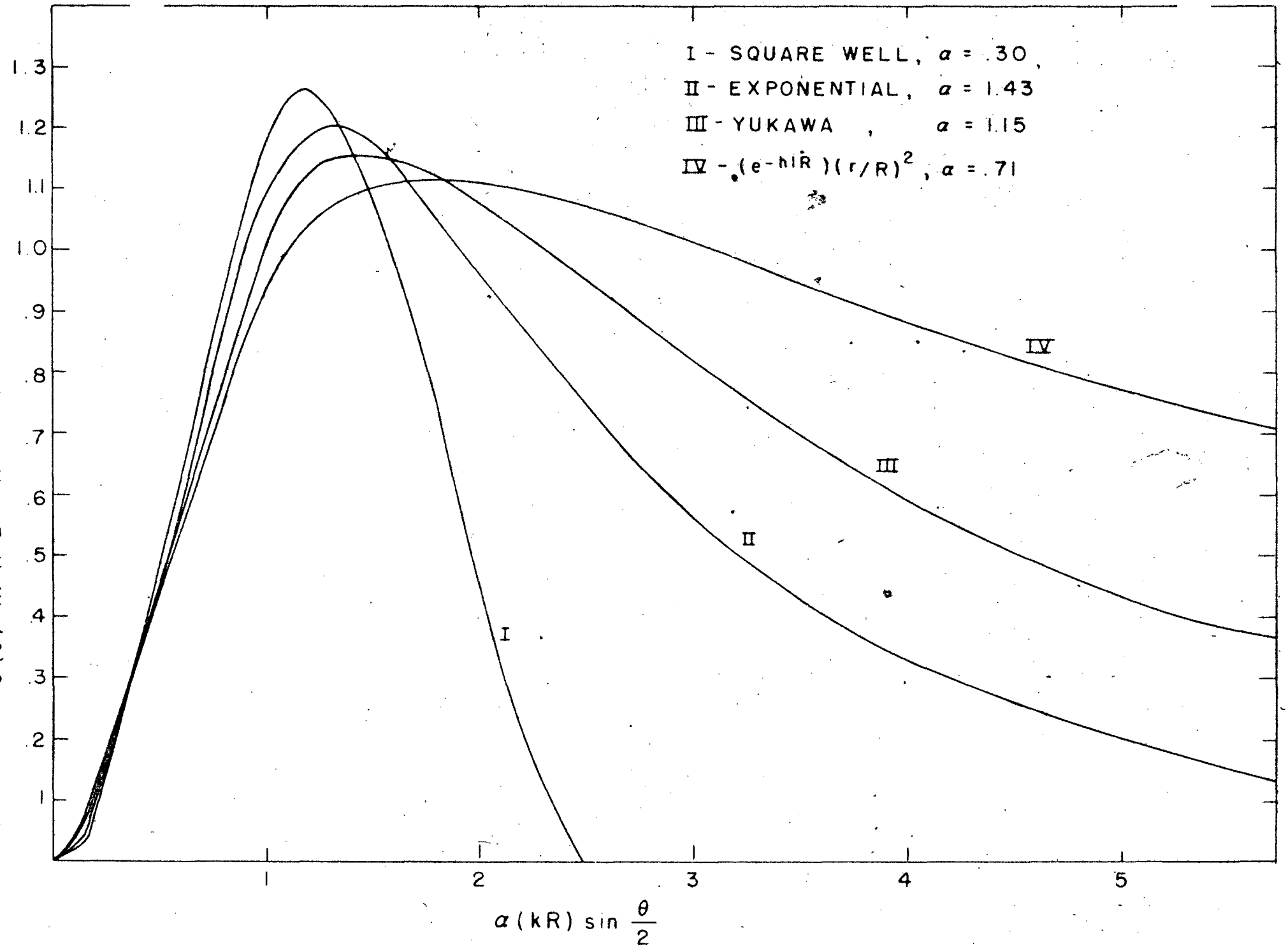
I - SQUARE WELL, α = .30
II - EXPONENTIAL, α = 1.43
III - YUKAWA, α = 1.15
IV - (e^-hR)(r/R)^2, α = .71
I
II
III
IV
1.3
1.2
1.1
1.0
.9
.8
.7
.6
.5
.4
.3
.2
1
1
2
3
4
5
α (kR) sin θ/2

FIG. 12

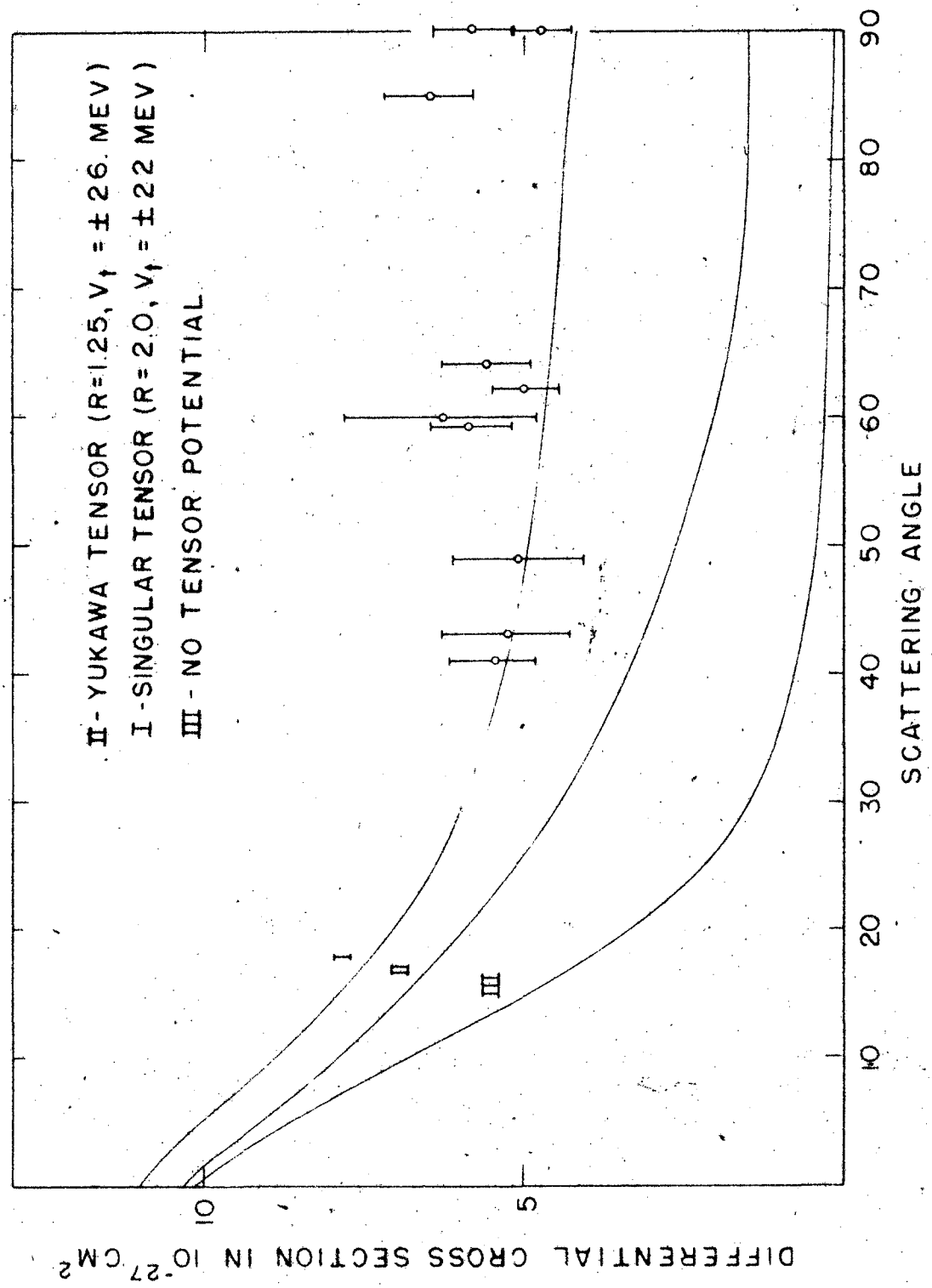
II - YUKAWA TENSOR (R=1.25, V_t = ± 26 MEV)
I - SINGULAR TENSOR (R = 2.0, V_t = ± 22 MEV)
III - NO TENSOR POTENTIAL
I
II
III
10
20
30
40
50
60
70
80
90
SCATTERING ANGLE
10
5
DIFFERENTIAL CROSS SECTION IN 10^{-27} CM^2

FIG. 13

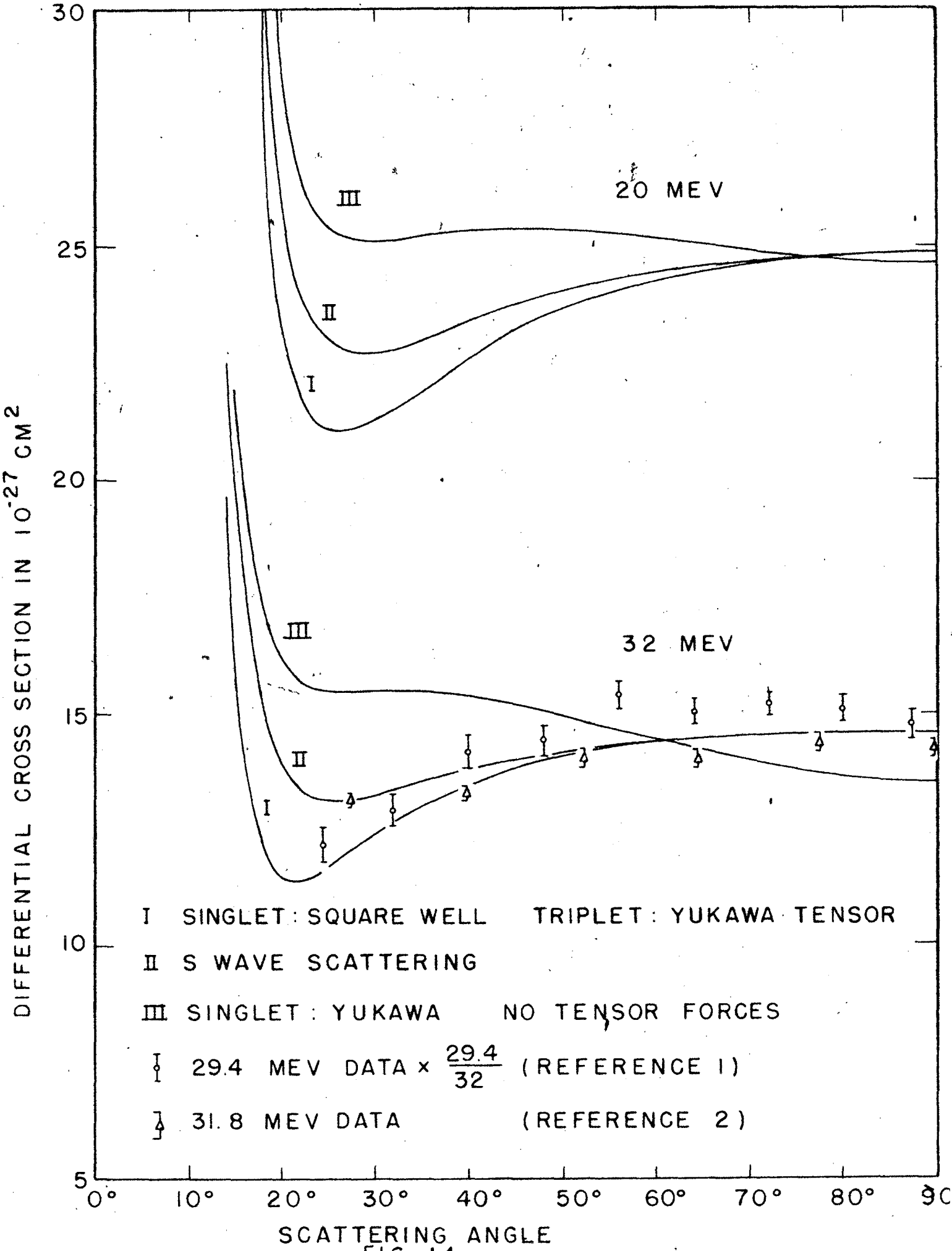
30
25
20
15
10
5
DIFFERENTIAL CROSS SECTION IN 10^{-27} CM^2
0°
10°
20°
30°
40°
50°
60°
70°
80°
90
SCATTERING ANGLE
20 MEV
32 MEV
III
II
I
I SINGLET: SQUARE WELL TRIPLET: YUKAWA TENSOR
II S WAVE SCATTERING
III SINGLET: YUKAWA NO TENSOR FORCES
29.4 MEV DATA × $\frac{29.4}{32}$ (REFERENCE 1)
31.8 MEV DATA (REFERENCE 2)

FIG. 14

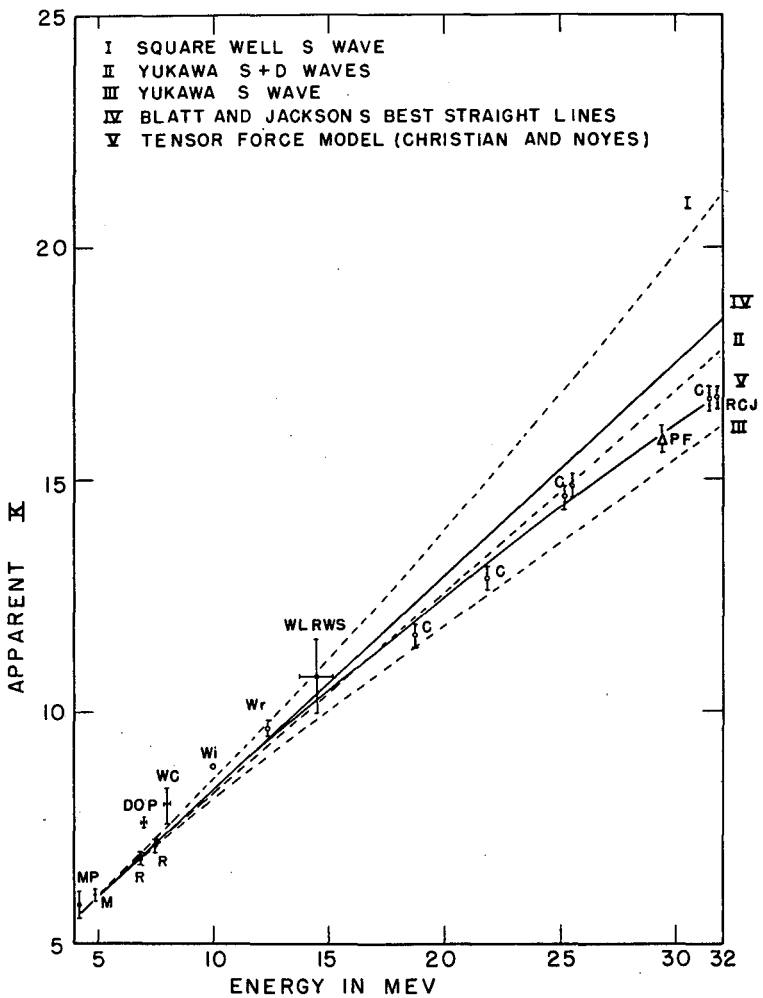
I SQUARE WELL S WAVE
II YUKAWA S+D WAVES
III YUKAWA S WAVE
IV BLATT AND JACKSON'S BEST STRAIGHT LINES
V TENSOR FORCE MODEL (CHRISTIAN AND NOYES)
APPARENT K
ENERGY IN MEV
25
20
15
10
5
5
10
15
20
25
30
32
I
IV
II
V
III
C
RCJ
PF
C
C
C
WL RWS
Wr
Wi
WC
DOP
R
R
MP
M

FIG 15

MU 245

II. The Production of Mesons By Protons on Deuterons

INTRODUCTION

The purpose of this paper is to attempt to predict the energy and angular distribution of mesons resulting from the bombardment of deuterium by 345 Mev protons, under the assumption that the cross section for the production of mesons in two nucleon collisions is known. Alternatively, since neutron sources of sufficient energy for the study of the production of mesons in n-p collisions are not readily available, this analysis can offer a method for learning something of this cross section. The production of mesons in proton-proton collisions is being investigated experimentally by Richman, Wilcox, Whitehead, Cartwright, and V. Peterson;[1] Keith Brueckner has conducted a theoretical investigation of the problem in the light of these experiments.[2]

The general method of attacking the problem was suggested to me by Professor Chew, in analogy with an approach he is using in the study of n-d inelastic scattering.[3] It rests upon two assumptions, of which the first is probably justified, while the second is open to considerable question. The first assumption is that the production takes place in a time so short compared to the period of the deuteron that the impulse approximation may be used. Since for the incident proton $v/c = .682$, the time for it to cross a meson compton wavelength is only 2 percent of the deuteron period. Hence it seems reasonable to assume that the problem can be treated in terms of the production of mesons by two nucleons, one of which has the momentum distribution of a particle in the deuteron, while the third particle simply carries off the complementary momentum without otherwise entering the reaction. The general examination of the errors made in impulse approximations of this type is to be discussed in a forthcoming paper by Professors Wick and Chew.

The more dubious assumption is that the particles which produce the meson do not then interact with the third particle except in so far as the exclusion principle limits the states available to them. This is essentially the same approximation as the neglect of double scattering off alternate particles in the inelastic scattering of nucleons by deuterons. In the latter problem one of the three particles must have a large momentum relative to a pair of particles that are interacting strongly. As Professor Chew has shown, this allows a straightforward treatment in terms of two body interactions. When a meson is formed, however, it is quite possible for all three nucleons to have comparable momenta, so that exact treatment would require a solutionof the three body problem.

Still, it can be argued that the situation is not so desparate as to invalidate the method used below. Firstly, when the three momenta are comparable, the exclusion principle causes a compensating reduction in the cross section. A further limitation occurs in that the phase space available to the three particles in this energy region (i.e. the region of high meson energy) is small. Outside this region the effect is small. In fact if the third particle has a relative energy of 40 Mev or greater, as is true on the average for most of the distribution except the high energy tail already discussed, its cross section at the average distance from the two interacting particles (4 or 5 wavelengths at this energy) covers less than 6 percent of the solid angle into which these particles may go. Moreover, the interaction between the two particles which produce the meson can be taken into account to the same extent as was done by Brueckner. This interaction completely alters the two nucleon distribution both in magnitude and shape; it increases the magnitude of the p-d cross section by a corresponding amount but has much less influence on the shape. Thus the results given below should be at least qualitatively correct, except possibly for the high energy tail. Clearly this method ignores the possibility of the formation of a

triton, but the results indicate that this process should be separable experimentally from the main body of the distribution.

DERIVATION OF THE SCATTERING MATRIX

The formal statement of the above assumptions and derivation of the scattering matrix will be carried out in terms of the R matrix notation.[3] The assumption that the two nucleon cross section is known can be stated as knowledge of appropriate two particle R matrices. These are then combined with the assumption that the third particle influences the reaction only by giving a deuteron momentum distribution to one of the interaction particles at some time previous to the production of the meson, to give an R matrix for the problem at hand.

In order to clarify the notation, I shall consider the two particle case briefly. Let the momentum and spin variables of the incident proton and struck neutron be denoted by ξ_o and ξ_n respectively, the final neutron variables by ξ_1 and ξ_2, and the positive meson variables by η^+. Then R^+_{np}, which describes the transformation of a proton ξ_o and a neutron ξ_n into two neutrons ξ_1 and ξ_2 and a positive meson η^+, may be written $(\xi_1\xi_2\eta^+|R^+_{np}|\xi_o\xi_n)$. Momentum conservation may be factored out giving

$$(\xi_1\xi_2\eta^+|R^+_{np}|\xi_o\xi_n) = \delta(\vec{k}_1+\vec{k}_2+\vec{q}-\vec{k}_o-\vec{h}_n)\left(\frac{\vec{k}_1-\vec{k}_2}{2}\sigma_1\sigma_2\vec{q}\,|r^+_{np}|\,\frac{\vec{k}_o-\vec{k}_n}{2}\sigma_o\sigma_n\right) \tag{1}$$

where the spin and momentum variables of the nucleons have been explicitly introduced. Note that this separation restricts us to treating the nucleons nonrelativistically throughout (except that the incident proton may be treated relativistically in calculating the energy and momentum available for the reaction; the treatment of the final nucleons can be shown to be a good approximation). The cross section for the production of positive mesons in an n-p collision is then to be written

$$d\sigma^+_{np} = \frac{2\pi}{\hbar v_o}|r^+_{np}|^2\delta(E_1+E_2+E_q-E_o-E_n)\frac{d\vec{k}'}{(2\pi)^3}\,\frac{d\vec{q}}{(2\pi)^3} \tag{2}$$

where $\vec{k}' = 1/2(\vec{k}_1-\vec{k}_2)$ and all other variables in r^+_{np} are to be expressed in terms of $\vec{k}'$, $\vec{q}$ (and $\vec{k}_o$) by means of momentum conservation. That is, formally, r^+_{np} appears in the cross section in the same way as a matrix element for the transition calculated in Born approximation; this analogy is useful in practice. In fact, the whole calculation is formally equivalent to a second order perturbation calculation assuming that the nuclear forces and meson production arise from separate interaction terms in the Hamiltonian and that the corresponding second order calculation for the two particle case gives the correct answer.

In terms of this notation the (unsymmetrized) R matrices for the deuteron problem under our assumptions may be written, for negatives:

$$(\xi_1\xi_2\xi_3\eta^-|R^-_{pd}|\xi_o\xi_D) = \sum_{\xi_o'\xi_n\xi_p} (\xi_1\xi_2\eta^-|R^-_{np}|\xi_o\xi_n)\delta_{\xi_p\xi_3} \times \psi_D(\xi_n\xi_p)\psi_{\xi_o}(\xi_o') \tag{3}$$

and for positives:

$$(\xi_1^{(n)}\xi_2^{(n)}\xi_3^{(p)}\eta^+|R^+_{pd}|\xi_o\xi_D) = \sum_{\xi_o'\xi_1\xi_2} \Big\{ e^{i\delta np}(\xi_1\xi_2\eta^+|R^+_{np}|\xi_o\xi_n)\delta_{\xi_p\xi_3}$$

$$+ e^{i\delta pp}(\xi_1^{(n)}\xi_3^{(p)}\ \eta^+|R^+_{pp}|\xi_o\xi_n)\delta_{\xi_n\xi_2}\Big\} \times \psi_D(\xi_n\xi_p)\psi_{\xi_o}(\xi_o') \tag{4}$$

where $\psi_{\xi_o}(\xi_o')$ is the incident plane wave $\delta_{\xi_o\xi_o'}$, $\psi_D(\xi_n\xi_p)$ is the deuteron function $\chi_D(\sigma_n\sigma_p)g_o\left(\frac{\vec{k}_n-\vec{k}_p}{2}\right)\delta(\vec{k}_n+\vec{k}_p-2\vec{k}_c)$, and $2\vec{k}_c$ is the momentum of the deuteron in whatever coordinate system is chosen. These two equations onctain the formal statement of the assumptions (a) that the third particle influences the production of the meson only through giving to the struck particle a deuteron momentum distribution at some time previous to the collision, and (b) that the three nucleons go directly into the final state $\xi_1\xi_2\xi_3$ without further interaction not contained in the two nucleon $R^{\pm}_{pn}$ and R^+_{pp}. According to the argument given in the introduction the interaction thus included should contain most of the influence of forces

between the particles in the final state. (3) is to be antisymmetrized in the three final neutrons $\xi_1\xi_2\xi_3$, and (4) in the two final neutrons; the corresponding r matrices are then to be squared, averaged over the initial proton and deuteron spin states, and summed over the final spin states. Note that the phase in the production of positives can be determined only from a specific meson theory so that the results will be uncertain by the amount of the interference term if empirical R matrices are used. The cross section is then given by

$$d\sigma_{pd} = \frac{2\pi}{\hbar v_o} |r_{pd}|^2 \delta(E_1+E_2+E_3+E_q-E_o-E_D)\rho_f$$

where the variables appearing in r_{pd} and in the density of final states ρ_f are to be interpreted in terms of the new momentum conservation condition $\vec{k}_1+\vec{k}_2+\vec{k}_3+\vec{q}-\vec{k}_o-2\vec{k}_c = 0$ that arises from integrating the original $\delta(\vec{k}_1+\vec{k}_2+\vec{q}-\vec{k}_o-\vec{k}_n)$ over $\vec{k}_n$ and $\vec{k}_p$.

Positive mesons can also be formed with the final nucleons coming off as a neutron and a deuteron instead of as two neutrons and a proton. According to the approximation being used here, this process will occur mainly when the positive meson is produced off the proton in the deuteron. This is the same process as that considered by Brueckner in proton-proton collisions, and can be included by calculating

$$(\xi_1\xi_D,\eta^+ \left|R^{+(d)}_{pd}\right| \xi_o\xi_D) = \sum_{\xi_o'\xi_n\xi_p} (\xi_D,\eta^+ \left|R^{+(d)}_{pp}\right| \xi_o\xi_p)\delta_{\xi_n\xi_1} \times \psi_D(\xi_n\xi_p)\psi_{\xi_o}(\xi_o') \qquad (5)$$

Clearly this term is incoherent with processes that lead to one proton and two neutrons. The alternative case when one of the two neutrons produced in the n-p collision picks up the original proton in the deuteron is neglected in this approximation. (3), (4), and (5) are the formal solution of the problem posed; given the R matrices for the production of mesons in two nucleon collisions, which except for phase may be learned empirically, they enable us to calculate

the production of mesons by proton-deuteron collisions under the assumptions (a) and (b) above, and subject to the uncertainty in the sign and magnitude of the coefficient of the interference term in the production of positives introduced by the unknown phase $e^{i(\delta_{pn}-\delta_{pp})}$.

RESULTS

The calculation of the phase space integrals and the matrix elements is discussed in the Appendix. Clearly (3), (4), and (5) imply a much more detailed knowledge of the production process than is at present available, so that simplifying assumptions have been introduced. These are general features found to hold for the four mesons theories considered by Brueckner, namely scalar, vector, and pseduoscalar with pseudoscalar and pseudovector coupling. These are (a) that the two particle matrix elements depend at most on the initial spins of the particles, the final spins and relative momenta, and the meson variables, and (b) that when the two final particles are identical, the final state is a singlet spin state. These restrictions arise from neglecting terms of order v/c of the meson velocity in the center of mass system. This is not a particularly good approximation, but leads to results capable of explaining the observed positive meson production, so will be used here as a semi-empirical result.

Under these restrictions, the transition rate for the production of negative mesons in p-d collisions is given by

$$
\begin{aligned}
w^-_{pd} = \frac{2\pi}{\hbar}\rho_f \times \frac{1}{6}\Big\{ & |M^-_{pn}(|k_1-k_2|^2,\eta^-)|^2 g_o^2(k_3+k_c) \\
& - M^-_{pn}(|k_1-k_2|^2,\eta^-)^* M^-_{pn}(|k_2-k_3|^2,\eta^-) g_o^*(k_3+k_c) g_o(k_1+k_c) \\
& + |M^-_{pn}(|k_2-k_3|,\eta^-)|^2 g_o^2(k_1+k_c) \\
& - M^-_{pn}(|k_2-k_3|^2,\eta^-)^* M^-_{pn}(|k_3-k_1|^2,\eta^-) g_o^*(k_1+k_c) g_o(k_2+k_c) \\
& + |M^-_{pn}(|k_3-k_1|^2,\eta^-)|^2 g_o^2(k_2+k_c) \\
& - M^-_{pn}(|k_3-k_1|^2,\eta^-)^* M^-_{pn}(|k_1-k_2|^2,\eta^-) g_o^*(k_2+k_c) g_o(k_3+k_c)\Big\}
\end{aligned}
\qquad (6)
$$

where M^-_{pn} is the two nucleon matrix element for the production of negatives and g_o is the momentum aplitude in the deuteron. The three positive terms give the distribution that would be produced in an n-p collision where the neutron had the momentum distribution in the deuteron. The negative terms are a correction taking account of those states which are excluded by the presence of the third particle. The assumption that M^-_{pn} is a constant gives the phase space for the problem less the exclusion principle correction. The meson distribution in the forward direction under this assumption is plotted in Figure 1 to the same scale as the production of negative mesons in n-p collisions under the same assumption. The general character of this distribution persists when the forces between the two interacting nucleons in their final state are taken into account.

The experimental results on the production of positive mesons in proton-proton collisions[1] is clearly incompatible with the assumption that the matrix element is a constant. Brueckner has shown that the discrepancy can be removed by taking into account the interaction of the nucleons after the production of the meson. Essentially this is found to introduce into the R matrix a factor $K_o/(\alpha_t^2+k_r^2)^{1/2}$ if the final state is a triplet, and $0.876\ K_o/(\alpha_s^2+k_r^2)^{1/2}$ if the final state is a singlet. ($\alpha^2 = \frac{M|\epsilon|}{\hbar^2}$ where ϵ is the binding energy of the deuteron or of the virtual singlet level for triplet and singlet states respectively, $\vec{k}_r = \frac{1}{2}(\vec{k}_1-\vec{k}_2)$ is the relative momentum of the final nucleons, and K_o is the inverse Compton wavelength of the meson $\mu c/\hbar$). Since under our assumptions the final state in the production of negatives is a singlet, the result (relative to the two nucleon production) is the same for all four theories and is given in Figure 2. The chief effect upon the deuteron spectrum (outside of the change in magnitude) of taking this effect into account is to shift the peak of the distribution from 40 Mev to 60 Mev. Coulomb forces between the two protons in the final state might be expected to wipe out the sharp peak in the two particle

distribution, but since little area is included under the peak, the smoothed out deuteron distribution should be little effected by this correction. Further, α_s is well known from p-p scattering, so that this result should be relatively trustworthy. In particulcar it is not subject to the interference correction that appears in the production of positive mesons.

The production of positives is more complicated in that a deuteron may appear as one of the final particles, that the final state may be singlet, triplet, or a mixture depending upon the theory, and that positives produced off the neutron may interfere with positives produced off the proton with an undetermined phase. The general formula for the case of a deuteron appearing as a final particle has already been given; the calculation is straighforward and leads to the result given in the Appendix. For the rest of the cross section the transition probability is

$$
\begin{aligned}
w^{+}_{pd} = \frac{2\pi}{\hbar}\rho_f \Big\{ & \left|M^{+}_{pn}(|k_1-k_2|^2,\eta^{+})\right|^2 g_o^2(k_3+k_c) \\
& + \left|M^{+}_{pp}(|k_1-k_3|^2,\eta^{+})\right|^2 g_o^2(k_2+k_c) \\
& + \left|M^{+}_{pp}(|k_2-k_3|^2,\eta^{+})\right|^2 g_o^2(k_1+k_c) \\
& - M^{+}_{pp}(|k_1-k_3|^2,\eta^{+})^{*} M_{pp}(|k_2-k_3|^2,\eta^{+}) g_o^{*}(k_2+k_c) g_o(k_1+k_c) \\
& + A\cos(\delta_{pn}-\delta_{pp}) M^{+}_{pn}(|k_1-k_2|^2,\eta^{+})^{*} g_o^{*}(k_3+k_c) \big[M^{+}_{pp}(|k_1-k_3|^2,\eta^{+}) g_o(k_2+k_c) \\
& \qquad + M^{+}_{pp}(|k_2-k_3|^2,\eta^{+}) \big] g_o(k_1+k_c) \Big\} \qquad (7)
\end{aligned}
$$

where $A\cos\delta$ depends upon the theory. Note that for equal p-n and p-p matrix elements the exclusion correction is one-third the correction in the case of negatives. This is a specific example of a general argument given by Chew and Steinberger[5] to show that the exclusion correction will increase the positive negative ratio for the production of positive mesons in complex nuclei.

For the final state a singlet spin state (scalar or vector mesons, $A = 1$), under the usual assumption that the n-p and p-p scattering lengths are equal,

the production of positives can also be obtained from Figure 2. Curve II times the ratio of n-p $\rightarrow \pi^+$ to n-p $\rightarrow \pi^-$ matrix elements (squared) gives the production off the neutron. Twice Curve II (since either proton can give a positive) times the square of the ratio of p-p $\rightarrow \pi^+$ to n-p $\rightarrow \pi^+$ matrix elements gives the production off the proton. The exclusion correction is the same as that taking II into III times the p-p to n-p ratio (squared). Under the assumption that both ratios are one the positive-negative ratio at 60 Mev in the forward direction is $3.84 \pm .84$. The uncertainty is due to the interference correction, which is of the same general form as the exclusion correction. The distribution is plotted in Figure 3.

For the final state a triplet (pseudoscalar theory with pseudovector coupling or 2/3 of the time with pseudoscalar coupling) the cross section is greatly increased by the possibility of the formation of a deuteron in the final state. The production off the proton is much the same as when the final state is a singlet, but the case when a deuteron appears as one of the final particles has comparable cross section. The comparison of these two parts of the cross section is given in Figure 4. Note that the value of the measured p-d cross section relative to the cross section measured for the production of positives in p-p collisions will depend critically upon the energy resolution of the apparatus used in the latter experiment. (The ratio of the deuteron peak to the peak of the continuum distribution is given by $4\pi\ E_d/\Delta E$ where E_d is the binding energy of the deuteron and ΔE is the energy resolution.) The production off the neutron still leads to two neutrons in a singlet state, so the interference term can be smaller. The total cross section (again assuming n-p and p-p

matrix element ratios equal to one, and neglecting interference) is plotted in Figure 5. The positive to negative ratio in the forward direction at 60 Mev is 8.22 $\pm$ .84. This large increase in the positive-negative ratio when the final state is a triplet is, of course, due to the added cross section resulting from the formation of a deuteron. It is clearly much larger than the uncertainty due to the inteference term. Hence, if the matrix element for p-n production were known to be approximately equal to that for p-p production, the experimental value for this positive-negative ratio would determine fairly clearly whether or not the formation of a deuteron occurs appreciably in p-p meson production. Conversely, if the formation of a deuteron could be demonstrated in p-p production, this ratio could give a fair idea of the ratio of p-n to p-p matrix elements (assuming the p-n matrix element symmetric between positive and negative meson production).

APPENDIX

A. Calculation of the Matrix Elements

The general expression (3) is pecialized by the assumption that R^-_{np} depends only on σ_1, σ_2, $(k_1-k_2)^2$, and η^- in the final state, σ_o and σ_n in the initial state, and is antisymmetric in σ_1 and σ_2. Performing the integrations, antisymmetrizing in the final three protons, and taking out the delta function giving momentum conservation gives

$$\begin{aligned} r^-_{pd} = \sum_{\sigma_n} & (\sigma_1\sigma_2|k_1-k_2|^2\eta^-|r^-_{np}|\sigma_o\sigma_n)\chi_D(\sigma_n\sigma_3)g_o(k_3+k_c) \\ & -(\sigma_1\sigma_3|k_1-k_3|^2\eta^- r^-_{np}|\sigma_o\sigma_n)\chi_D(\sigma_n\sigma_2)g_o(k_2+k_c) \\ & -(\sigma_3\sigma_2|k_3-k_2|^2\eta^-|r^-_{np}|\sigma_o\sigma_n)\chi_D(\sigma_n\sigma_1)g_o(k_1+k_c) \end{aligned} \tag{8}$$

Since we are only interested in the meson distribution, the result will be integrated over all nucleon momenta; hence the matrix element that will appear in the cross section may be written

$$\begin{aligned} |r^-_{pd}|^2 = \frac{1}{3!} \times \frac{1}{6} \times 3 \sum_{\substack{\sigma_o\sigma_n\sigma_n' D \\ \sigma_1\sigma_2\sigma_3}} & g_o^*(k_3+k_o)F^*(|k_1-k_2|^2,\eta^-)\chi_D^*(\sigma_n'\sigma_3)(\sigma_1\sigma_2|r^-_{np}|\sigma_o\sigma_n')^* \\ & \times \Big\{(\sigma_1\sigma_2|r^-_{np}|\sigma_o\sigma_n)\chi_D(\sigma_n\sigma_3)F(|k_1-k_2|^2,\eta^-)g_o(k_3+k_c) \\ & - 2(\sigma_3\sigma_2|r^-_{np}|\sigma_o\sigma_n)\chi_D(\sigma_n\sigma_1)F(|k_3-k_2|^2,\eta^-)g_o(k_1+k_c)\Big\} \end{aligned} \tag{9}$$

where (as is the case in the theories considered by Brueckner) the momentum dependence can be factored out as $F(|k_i-k_j|^2,\eta^-)$, the $\frac{1}{3}!$ is the phase space factor for three identical particles, and the 1/6 comes from the average over the six initial spin states. Since

$$\sum_{D,\sigma_3} \chi_D^*(\sigma_n'\sigma_3)\chi_D(\sigma_n\sigma_3) = \frac{3}{2}\delta_{\sigma_n\sigma_n'} \tag{10}$$

the diagonal term reduces to

$$\frac{1}{2}g_o^2(k_3+k_c) \times \frac{1}{4}\sum_{\substack{\sigma_o\sigma_n\\ \sigma_1\sigma_2}} |F(|k_1-k_2|^2,\eta^-)(\sigma_1\sigma_2|r_{np}^-|\sigma_o\sigma_n)|^2$$

$$= \frac{1}{2}g_o^2(k_3+k_c)\,|M_{np}^-(|k_1-k_2|^2,\eta^-)|^2 \qquad (11)$$

i.e. simply to 1/2 the matrix element (squared) for negative production in p-n collisions times the momentum distribution in the deuteron. This is the term to be expected for direct production off the neutron. (The 1/2 occurs in the two particle case also as the phase space factor for two identical particles.) Similarly the spin sum for the exclusion correction gives

$$\frac{1}{2}g_o^*(k_3+k_c)g_o(k_1+k_c)M_{pn}^-(|k_1-k_2|)^2,\eta^-)*M_{pn}^-(|k_2-k_3|^2,\eta^-) \qquad (12)$$

so that the exclusion correction is 100 percent when the three final particles all have the same momenta, as it should be. Combining these and including the cyclic permutations of 1,2,3 gives the result (6) already quoted. The matrix element for positives, (7), is obtained in the same way. Here, however, no simplification such as the final state being always a singlet occurs and different theories can give different results for the coefficient of the interference term $A\cos(\delta_{pn}-\delta_{pp})$.

B. Phase Space Integrations

The canonical variables picked were r, the internal coordinate of the deuteron, y, the distance between the incident proton and the center of mass of the deuteron, and x, the center of mass coordinate for the three particles. The momenta conjugate to these coordinates are $\vec{k}_r = \frac{1}{2}(\vec{k}_2-\vec{k}_3)$ with $m = \frac{1}{2}M$, $\vec{k}_y = \frac{1}{3}(2\vec{k}_1-\vec{k}_2-\vec{k}_3)$, with $m = \frac{2}{3}M$, and $\vec{k}_x = \frac{1}{3}(\vec{k}_1+\vec{k}_2+\vec{k}_3)$ with $m = 3M$. Hence the energy in the final state is

$$\frac{\hbar^2 k_r^2}{M} + \frac{3\hbar^2 k^2}{4M} + \frac{\hbar^2 k_x^2}{6M} + E_q$$

where E_q is the total meson energy $(\mu^2 c^4 + c^2\hbar^2 q^2)^{1/2}$, and the initial energy is $T_o - E_d$ were T_o is the kinetic energy of the incident proton and E_d the binding energy of the deuteron. T_o must be calculated relativistically (and $\vec{k}_o$), but the final nucleons may be treated as non-relativistic even in the laboratory system without making much error in the meson distribution. For the two particle case, however, the distribution must be calculated in the center of mass system where the final nucleons can be treated non-relativistically and then transformed relativistically to the laboratory system. Since $\frac{dE_f}{dk_r} = \frac{2\hbar^2 k_r}{M}$ the density of final states is

$$\rho_f = \frac{1}{dE_f} \frac{d\vec{k}_r}{(2\pi)^3} \frac{d\vec{k}_y}{(2\pi)^3} \frac{d\vec{q}}{(2\pi)^3} = \frac{M}{2\hbar^2} k_r \frac{d\Omega_r}{(2\pi)^3} \frac{d\vec{k}_y}{(2\pi)^3} \frac{d\vec{q}}{(2\pi)^3} \tag{13}$$

Conservation of momentum requires that $\vec{k}_x + \vec{q} = \vec{k}_o$, so that the conservation of energy equation may be solved for k_r in terms of k_y and known quantities independent of the nucleon angles (the reason for this choice of variables) giving

$$k_r = \frac{1}{\hbar}\sqrt{MT_o - ME_d - ME_q - \frac{\hbar^2}{6}(\vec{k}_o - \vec{q})^2 - \frac{3}{4}\hbar^2 k_y^2} \cong \quad g - \frac{3}{4}k_y^2 \tag{14}$$

For a constant matrix element the diagonal term leads to the integral

$$\int \rho_f g_o^2(k_1) = \frac{d\vec{q}}{(2\pi)^3} \int_o^{\sqrt{\frac{4g}{3}}} \frac{M\sqrt{g - \frac{3}{4}k_y^2}\, k_y^2 dk_y}{2\hbar^2 (2\pi)^3} 8\pi^2 \int_{-1}^{1} \frac{dM_y}{(2\pi)^3} \frac{8\pi\alpha N^2}{(\alpha^2 + \frac{1}{9}k_x^2 + k_y^2 + \frac{2}{3}k_x k_y M_y)^2} \tag{15}$$

where the deuteron momentum amplitude has been taken to be $\frac{\sqrt{8\pi\alpha N^2}}{\alpha^2 + k^2}$. The calculation has also been carried through for the more reasonable deuteron wave function $(e^{-\alpha r} - e^{-\beta r})/r$ with $\beta/\alpha = 6$. The only important difference this makes over the wave function $\frac{e^{-\alpha r}}{r}$ is that N^2 changes

from one to $6(6+1)/(6-1)^2 = 1.68$. The angular integration is elementary leading to the result

$$\frac{d\vec{q}}{(2\pi)^3}\frac{\sqrt{3}MN^2\alpha}{\pi h^2}\int_0^1 \frac{\sqrt{x(1-x)}\,dx}{(a^2+b^2)^2 + 2(a^2-b^2)x + x^2} \tag{16}$$

where we have introduced the dimensionless quantities $a^2 = \frac{3}{4}\frac{\alpha^2}{g}$ and $b^2 = \frac{1}{12}\frac{k_x^2}{g}$ and x is dimensionless. The branch points at the two ends of the path of integration allow this integral to be converted into a contour integral and evaluated by residues giving

$$\pi\left\{\frac{a\left[\sqrt{(1+a^2-b^2)^2+4a^2b^2} - (1+a^2-b^2)\right]^{1/2} + b\left[\sqrt{(1+a^2-b^2)^2+4a^2b^2} + (1+a^2-b^2)\right]^{1/2}}{2\sqrt{2}\,ab} - 1\right\} \tag{17}$$

and

$$\int \rho_f g_o^2(k_1) =$$

$$\frac{d\vec{q}}{(2\pi)^3}\frac{\sqrt{3}MN^2\alpha}{h^2}\left\{\frac{A\left[\sqrt{(G+A^2-B^2)^2+4A^2B^2}-(G+A^2-B^2)\right]^{\frac{1}{2}}+B\left[\sqrt{(G+A^2-B^2)^2+4A^2B^2}+(G+A^2-B^2)\right]^{\frac{1}{2}}}{2\sqrt{2}\,AB} - 1\right\} \tag{18}$$

where $A^2 = \frac{3}{4}\frac{\alpha^2}{K_o^2}$, $B^2 = \frac{1}{12}\frac{k_x^2}{K_o^2}$, $G = \frac{g}{K_o^2}$ and K_o is the meson inverse Compton wave length. This reduces to the corresponding result for the two particle distribution as the binding energy goes to zero, and to zero as the binding energy becomes infinite. The exclusion principle correction reduces to

$$\frac{d\vec{q}}{(2\pi)^3}\frac{3MN^2\alpha}{2\pi h^2}\frac{K_o}{k_x}\int_0^{\sqrt{\frac{4}{3}G}} x\,dx \int_{\frac{1}{3}\frac{k_x}{k_o}-\frac{1}{2}x}^{\frac{1}{3}\frac{k_x}{k_o}+\frac{1}{2}x} dy\,\frac{K_o^2 \log\frac{\alpha^2+(K_oy+k_r)^2}{\alpha^2+(K_oy-k_r)^2}}{\alpha^2+K_o^2y^2+k_r^2} \tag{19}$$

$\left(\text{where } \frac{k_r^2}{K_o^2} = \frac{4}{3}G - x\right)$, which was evaluated numerically. The diagonal term integral that occurs when the forces between the particles in the final state are taken into account differs only by the factor $K_o^2/(\alpha_i^2+k_r^2)$ in the final integration so that this integral may again be done by residues giving

$$\int \frac{\rho_f g_o^2(k_1)K_o^2}{\alpha_i^2+\frac{1}{4}(k_2-k_3)^2}$$

$$= \frac{d\vec{q}}{(2\pi)^3} \frac{\sqrt{3}MN^2\alpha K_o^2}{h^2\left[(G+A^2-B^2+A_i^2)^2 + 4A^2 B^2\right]} \times$$

$$\left\{(G+A^2-B^2+A_i^2)\left[\frac{A\left[\sqrt{(G+A^2-B^2)^2+4A^2B^2}-(G+A^2-B^2)\right]^{\frac{1}{2}}+B\left[\sqrt{(G+A^2-B^2)^2+4A^2B^2}+(G+A^2-B^2)\right]^{\frac{1}{2}}}{2\sqrt{2}\,AB}\right]\right.$$

$$+\frac{1}{\sqrt{2}}\left[B\left[\sqrt{(G+A^2-B^2)^2+4A^2B^2}-(G+A^2-B^2)\right]^{\frac{1}{2}}-A\left[\sqrt{(G+A^2-B^2)^2+4A^2B^2}+(G+A^2-B^2)\right]^{\frac{1}{2}}\right]$$

$$\left.-A_i\sqrt{G+A_i^2}\right\} \tag{20}$$

where $A_i^2 = \frac{\alpha_s^2}{K_o^2}$ or $\frac{\alpha_t^2}{K_o^2}$ depending upon whether the final state is a singlet or a triplet. The corresponding exclusion principle correction was not calculated because of mathematical difficulties, but was estimated to be approximately the same percent of the diagonal term at the same meson energy as the corresponding correction for the constant matrix element case, since the general form of the diagonal term was so little altered by the inclusion of the interaction between the two final particles.

When one of the final particles is a deuteron the energy conservation condition becomes

$$E_f = \frac{\hbar^2 k_x^2}{GM} + \frac{2\hbar^2 k_y^2}{4M} + E_q = T_o$$

while the momentum conservation condition remains unaltered, so that the density of final states is

$$\rho_f = \frac{2M}{3\hbar^2} k_y \frac{d\Omega_y}{(2\pi)^3} \frac{d\vec{q}}{(2\pi)^3} \quad \text{where} \quad k_y = \frac{2}{\sqrt{3}}\sqrt{g+\alpha_t^2} \tag{21}$$

The angular integration is elementary, giving

$$\int d\Omega_y g_o^2(k_1) \doteq \frac{9\pi N^2}{4\left[(G+A^2-B^2+A_t^2)^2+4A^2B^2\right]^2} \tag{22}$$

The ratio of matrix elements for the two particle case is given by Brueckner as

$$\left|\frac{M_{pp}^{+}}{M_{pp}^{+}\sqrt{\alpha^2+k_r^2}}\right|^2 = \frac{(2\pi)^3\left|\sqrt{\frac{\alpha}{2\pi}}\,K_o\right|^2}{K_o^2} = 4\pi^2\alpha \tag{23}$$

so that this result can be immediately related to our previous formulae.

REFERENCES

(1) H. A. Wilcox, W. F. Cartwright, C. Richman, and M. N. Whitehead, Bul. Am. Phys. Soc., No. 3, B-10, (1950)
C. Richman and H. A. Wilcox, Phys. Rev., (to be published) and private communication.
V. Peterson, Phys. Rev., (to be published) and private communication.

(2) K. Brueckner, Phys. Rev., (to be published) and private communication.

(3) G. F. Chew, Phys. Rev., (to be published)

(4) C. Möller, Det. Kgl. Danshe Vidensk., XIII, Nr. 1 (1946)

(5) G. F. Chew and J. Steinberger, Phys. Rev. 78, 497 (1950)

FIGURE CAPTIONS

All curves are the cross section for meson production as a function of meson energy in the forward direction for 345 Mev protons incident. The reactions to which the cruves refer are given on the figures. p-n and p-p matrix elements are assumed equal. The absolute value is left arbitrary as it depends upon the strength of the coupling of the meson field to the nucleons, but relative normalization is correct. The following assumptions apply to the indicated figures:

Figure 1. Production of negative mesons; constant matrix element.

Figure 2. Production of negative mesons; singlet final state.

Figure 3. Production of positive mesons and negative mesons; singlet final state; interference term neglected.

Figure 4. Production of positives off the proton; triplet final state.

Figure 5. Production of positives and negatives; triplet final state when the final particles in the two particle interaction are not identical.

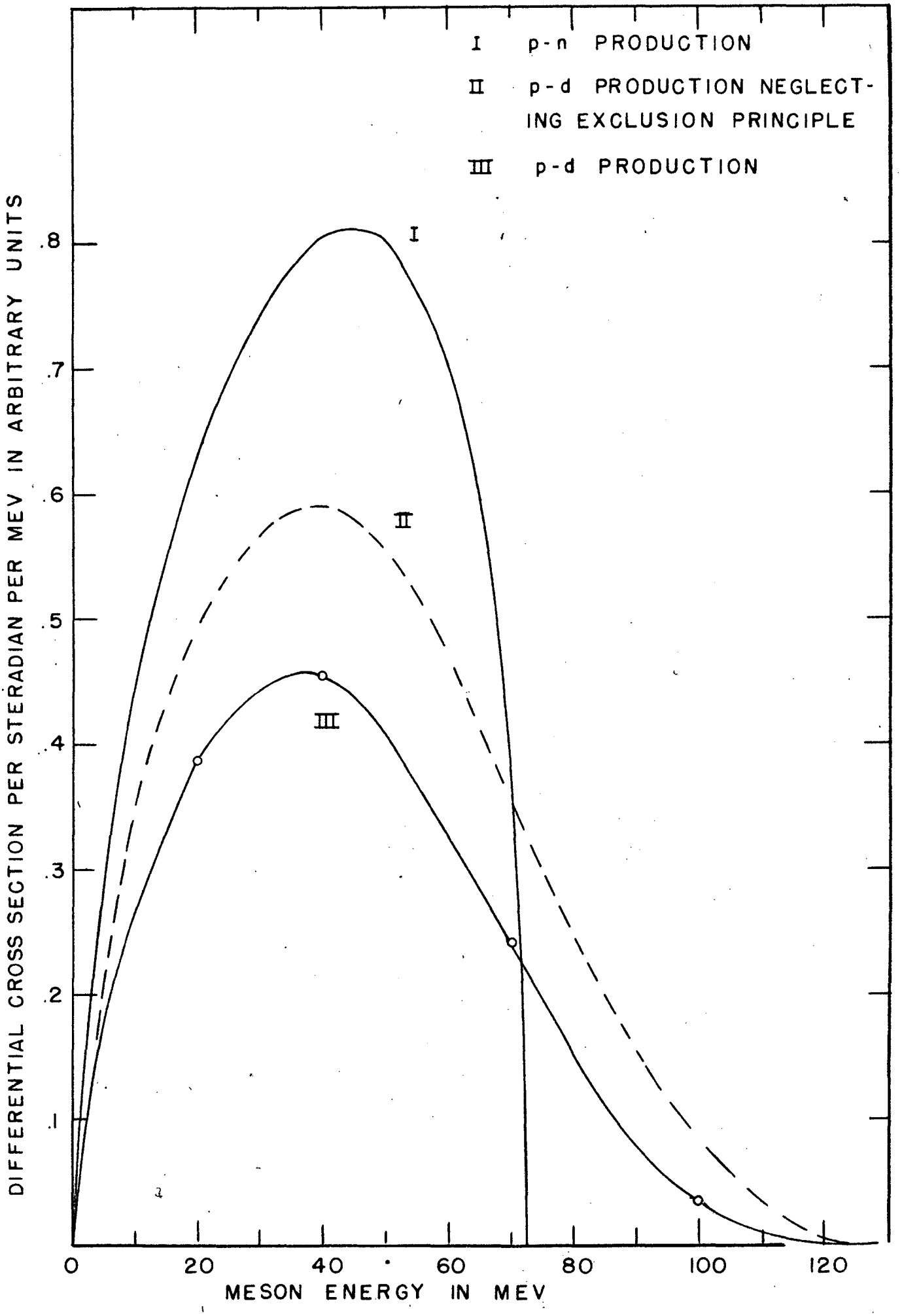
I p-n PRODUCTION
II p-d PRODUCTION NEGLECTING EXCLUSION PRINCIPLE
III p-d PRODUCTION
DIFFERENTIAL CROSS SECTION PER STERADIAN PER MEV IN ARBITRARY UNITS
.8
.7
.6
.5
.4
.3
.2
.1
I
II
III
0
20
40
60
80
100
120
MESON ENERGY IN MEV

FIG. 1

14961-1

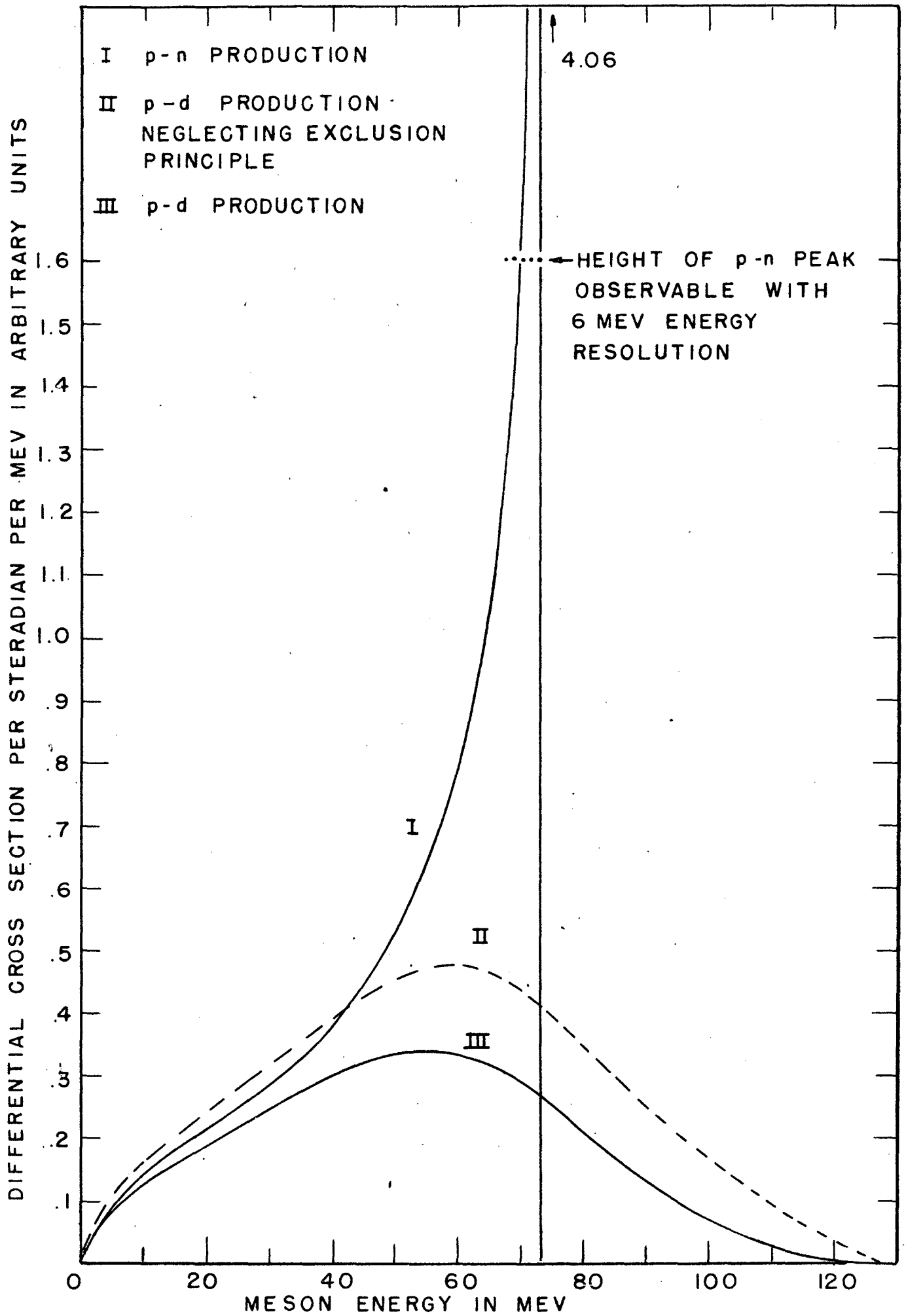
I p-n PRODUCTION
II p-d PRODUCTION NEGLECTING EXCLUSION PRINCIPLE
III p-d PRODUCTION
4.06
HEIGHT OF p-n PEAK OBSERVABLE WITH 6 MEV ENERGY RESOLUTION
DIFFERENTIAL CROSS SECTION PER STERADIAN PER MEV IN ARBITRARY UNITS
1.6
1.5
1.4
1.3
1.2
1.1
1.0
.9
.8
.7
.6
.5
.4
.3
.2
.1
I
II
III
0
20
40
60
80
100
120
MESON ENERGY IN MEV

FIG. 2

14962-1

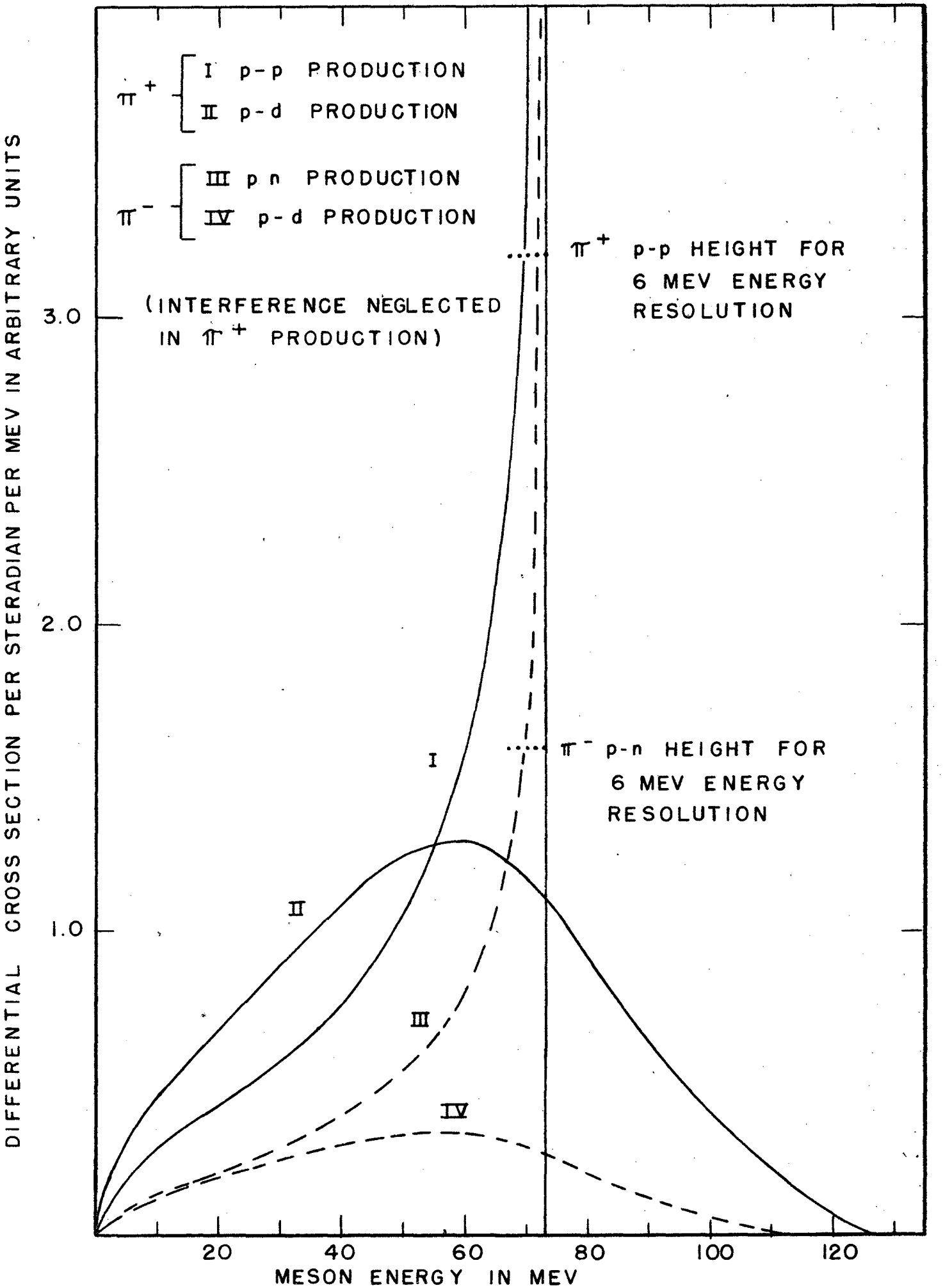
π+ I p-p PRODUCTION
II p-d PRODUCTION
π− III p n PRODUCTION
IV p-d PRODUCTION
(INTERFERENCE NEGLECTED IN π+ PRODUCTION)
π+ p-p HEIGHT FOR 6 MEV ENERGY RESOLUTION
π− p-n HEIGHT FOR 6 MEV ENERGY RESOLUTION
I
II
III
IV
3.0
2.0
1.0
20
40
60
80
100
120
DIFFERENTIAL CROSS SECTION PER STERADIAN PER MEV IN ARBITRARY UNITS
MESON ENERGY IN MEV

FIG. 3

14963-1

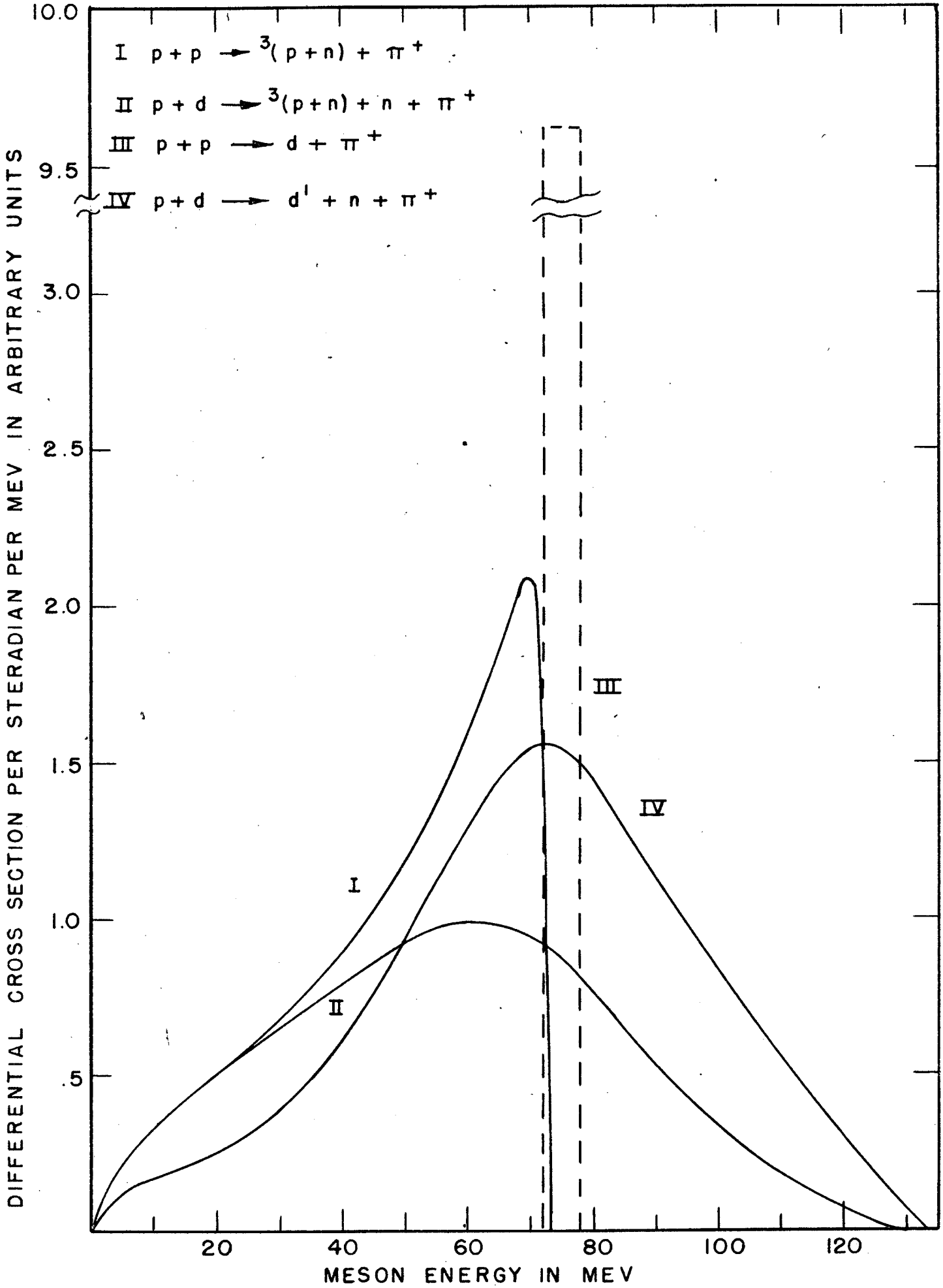
I p + p → 3(p + n) + π+
II p + d → 3(p + n) + n + π+
III p + p → d + π+
IV p + d → d' + n + π+
DIFFERENTIAL CROSS SECTION PER STERADIAN PER MEV IN ARBITRARY UNITS
10.0
9.5
3.0
2.5
2.0
1.5
1.0
.5
I
II
III
IV
20
40
60
80
100
120
MESON ENERGY IN MEV

FIG. 4

14964-

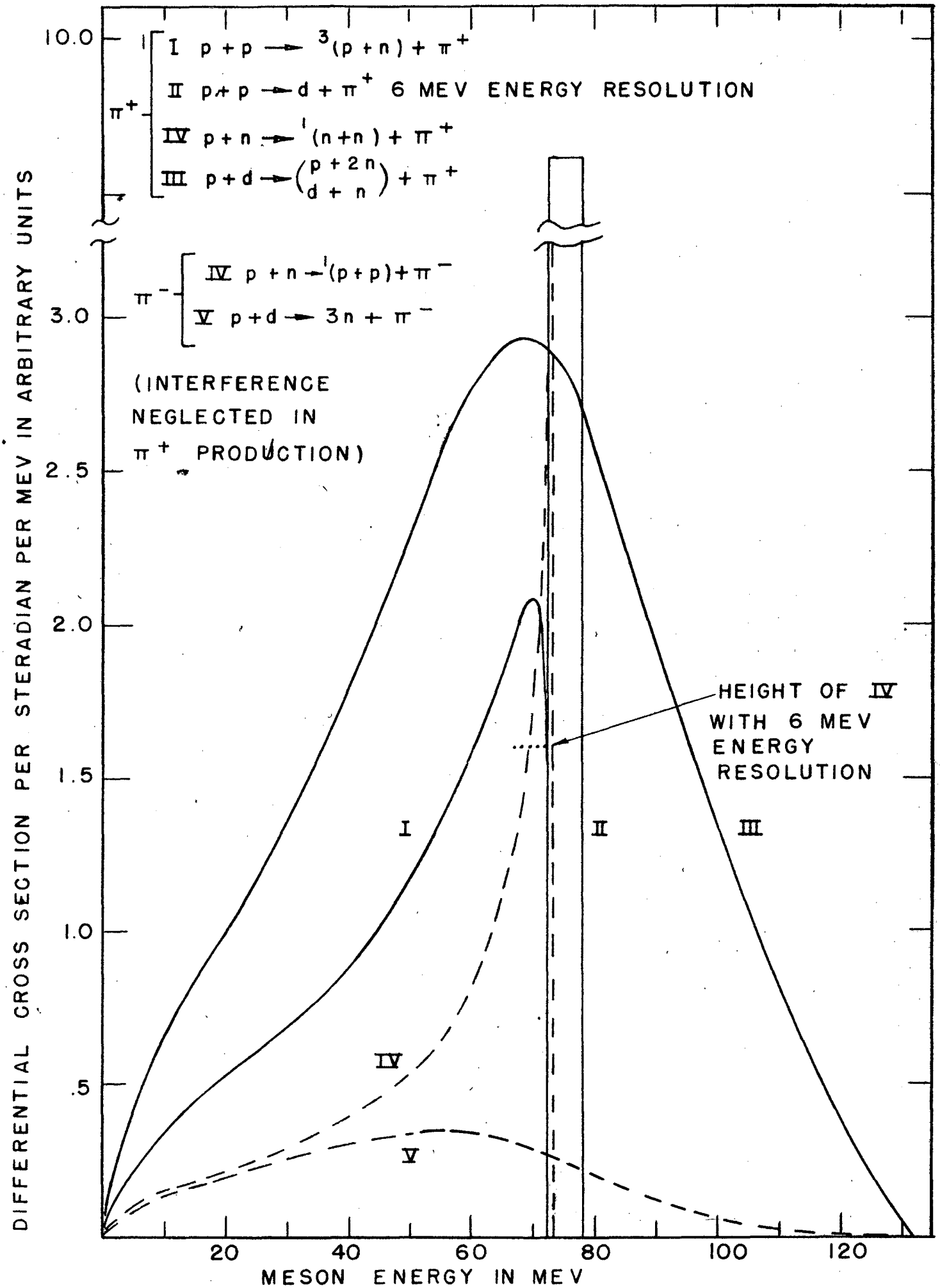
10.0
3.0
2.5
2.0
1.5
1.0
.5
π+
I p + p → 3(p + n) + π+
II p + p → d + π+ 6 MEV ENERGY RESOLUTION
IV p + n → 1(n + n) + π+
III p + d → (p + 2n / d + n) + π+
π−
IV p + n → 1(p + p) + π−
V p + d → 3n + π−
(INTERFERENCE NEGLECTED IN π+ PRODUCTION)
HEIGHT OF IV WITH 6 MEV ENERGY RESOLUTION
I
II
III
IV
V
20
40
60
80
100
120
MESON ENERGY IN MEV
DIFFERENTIAL CROSS SECTION PER STERADIAN PER MEV IN ARBITRARY UNITS

FIG. 5

14965-